

Official Journal of Turkish Society of Magnetic Resonance

# CRMRI

## Current Research in MRI

Pediatric Morel-Lavellée Lesions  
Fatihoğlu and Kadirhan

Histopathological Correlation of MpMRI  
and PIRADS Scores in Prostate Cancer  
Tonkaz and Şenbil

The Correlation between Diffusion Tensor  
Imaging-Histopathological Findings of Meningioma  
Alkan et al.

## Editor in Chief

Mecit Kantarcı 

Department of Radiology, Erzincan Binali Yıldırım University, Faculty of Medicine; Atatürk University, Faculty of Medicine, Erzincan, Erzurum, Turkey

## Editors

### Abdominal Radiology

Aytekin Oto 

The University of Chicago, Department of Radiology, Chief Physician, Head of the Faculty Practice Plan and Dean for Clinical Affairs, Chicago, USA

Murat Danacı 

Department of Radiology, Ondokuz Mayıs University, Faculty of Medicine, Samsun, Turkey

### Breast Radiology

Serap Gültekin 

Department of Radiology, Gazi University, Faculty of Medicine, Ankara, Turkey

### Cardiac Radiology

Memduh Dursun 

Department of Radiology, İstanbul University, İstanbul Faculty of Medicine, İstanbul, Turkey

Cihan Duran 

Department of Diagnostic and Interventional Imaging, The University of Texas, McGovern Medical School, Texas, USA

### Emergency Radiology

Mehmet Ruhi Onur 

Department of Radiology, Hacettepe University Faculty of Medicine Hospital, Ankara, Turkey

### Engineer Group

Esin Öztürk Işık 

Biomedical Engineering, Boğaziçi University, İstanbul, Turkey

### Head & Neck Radiology

Nafi Aygün 

Department of Radiology, Johns Hopkins University School of Medicine, Baltimore, Maryland, USA

Hatice Gül Hatipoğlu 

Department of Radiology, Health Science University, Gulhane Faculty of Medicine, Ankara Bilkent City Hospital, Ankara, Turkey

### Musculoskeletal Radiology

Nil Tokgöz 

Department of Radiology, Gazi University, Faculty of Medicine, Ankara, Turkey

### Neuroradiology Radiology


Alpay Alkan 

Department of Radiology, Bezmialem Vakıf University, Faculty of Medicine, İstanbul, Turkey

### Pediatric Radiology

Korgün Koral 

Department of Radiology, University of Texas Southwestern Medical Center, Dallas, TX, USA

Süreyya Burcu Görkem 

Department of Pediatric Radiology, Adana State Hospital, Adana, Turkey

### Thorax Radiology

Polat Koşucu 

Department of Radiology, Karadeniz Teknik University, Faculty of Medicine, Trabzon, Turkey

### Biostatistical Consultant

Sonay Aydın 

Department of Radiology, Erzincan Binali Yıldırım University, Faculty of Medicine, Erzincan, Turkey

Türk Manteyik Rezonans Derneği adına sahibi / Owner: Abdülmecit Kantarcı • Sorumlu Yazı İşleri Müdürü / Responsible Manager on behalf of the Turkish Society of Magnetic Resonance: Sonay Aydın • Yayın türü / Publication Type: Yerel süreli / Local periodical • Basım yeri / Printed at: Kaya Ozalit, Meclis-i Mebusan cad. Mimar Han No:75/A 34427 Fındıklı İstanbul, Turkey (+90 212 243 81 05) • Basım tarihi / Printing Date: Nisan 2022 / April 2022 • Türk Manteyik Rezonans Derneği tarafından yayınlanmaktadır / Published by Turkish Society of Magnetic Resonance, Konak Mah. 858. Sok. No:2 Çakıroğlu İş Hanı Kat:5 Daire:55 Konak / İzmir (+90 232 446 75 96)



#### Founder

İbrahim KARA

#### General Manager

Ali ŞAHİN

#### Publishing Directors

İrem SOYSAL

Gökhan ÇİMEN

#### Editor

Bahar ALBAYRAK

#### Publications Coordinators

Arzu ARI

Deniz KAYA

İrmak BERBEROĞLU

Alara ERGİN

Hira Gizem FIDAN

Vuslat TAŞ

İrem ÖZMEN

#### Web Coordinators

Sinem Fehime KOZ

Doğan ORUÇ

#### Finance Coordinator

Elif YILDIZ ÇELİK

#### Contact

Address: Büyükdere Cad. No: 105/9

34394 Mecidiyeköy, Şişli-İstanbul

Phone: +90 212 217 17 00

E-mail: info@avesyayincilik.com

## AIMS AND SCOPE

Current Research in MRI (Curr Res MRI) is a scientific, open access, online-only official publication of the Turkish Society of Magnetic Resonance published in accordance with independent, unbiased, and double-blinded peer-review principles. The journal is published triannually in April, August, and December. The publication language of the journal is English.

Current Research in MRI aims to contribute to the literature by publishing manuscripts at the highest scientific level on radiology. The journal publishes original articles, reviews, case reports, and letters to the editor that are prepared in accordance with ethical guidelines.

The target audience of the journal includes specialists, researchers and professionals who working and interested in the field of radiology.

The editorial and publication processes of the journal are shaped in accordance with the guidelines of the International Committee of Medical Journal Editors (ICMJE), World Association of Medical Editors (WAME), Council of Science Editors (CSE), Committee on Publication Ethics (COPE), European Association of Science Editors (EASE), and National Information Standards Organization (NISO). The journal is in conformity with the Principles of Transparency and Best Practice in Scholarly Publishing (doaj.org/bestpractice).

### Publication Fee Policy

All expenses of the journal are covered by the Turkish Society of Magnetic Resonance. Processing and publication are free of charge with the journal. No fees are requested from the authors at any point throughout the evaluation and publication process. All manuscripts must be submitted via the online submission system, which is available at <http://curremr.com>. The journal guidelines, technical information, and the required forms are available on the journal's web page.

### Advertisement Policy

Current Research in MRI can publish advertisement images in the journal's website upon the approval of the Editor in

Chief. Potential advertisers should contact the Editorial Office. Advertisers have no effect on the editorial decisions or advertising policies.

### Disclaimer

Statements or opinions expressed in the manuscripts published in the journal reflect the views of the author(s) and not the opinions of the editors, editorial board, and/or publisher; the editors, editorial board, and publisher disclaim any responsibility or liability for such materials.

### Open Access Statement

Current Research in MRI is an open access publication, and the journal's publication model is based on Budapest Access Initiative (BOAI) declaration. All published content is available online, free of charge at <http://curremr.com>. The journal's content is licensed under a Creative Commons Attribution-NonCommercial (CC BY-NC) 4.0 International License which permits third parties to share and adapt the content for non-commercial purposes by giving the appropriate credit to the original work.

You can reach the current version of the instructions to authors at <https://curremr.com/EN>

**Editor in Chief: Mecit Kantarcı**

**Address:** Department of Radiology, Erzincan Binali Yıldırım University School of Medicine, Erzincan, Turkey

**E-mail:** [akkanrad@hotmail.com](mailto:akkanrad@hotmail.com)

**Publisher: Turkish Society of Magnetic Resonance**

**Address:** Konak Mah. 858. Sok. No: 2 Çakıroğlu İş Hanı Kat: 5 Daire: 55 Konak / İzmir, Turkey

**Publishing Service: AVES**

**Address:** Büyükdere Cad., 105/9 34394 Şişli, İstanbul, Turkey

**Phone:** +90 212 217 17 00

**E-mail:** [info@avesyayincilik.com](mailto:info@avesyayincilik.com)

**Webpage:** [www.avesyayincilik.com](http://www.avesyayincilik.com)



## CONTENTS

### REVIEW ARTICLE

- 1 A Review on the Medical Applications of Functional Magnetic Resonance Imaging  
Bhagyalakshmi Akkavil Thondikandi, Arun Krishnan MP

### ORIGINAL ARTICLES

- 6 Magnetic Resonance Imaging Findings of Lower Extremity Morel-Lavellée Lesions in Pediatric Patients: A Preliminary Study  
Erdem Fatihoğlu, Özlem Kadirhan
- 10 Histopathological Correlation of Current Prostate Imaging Reporting and Data System Scores with 3 Tesla Multiparametric Prostate Magnetic Resonance Imaging in Detecting Prostate Cancer  
Gökhan Tonkaz, Düzgün Can Şenbil
- 15 Investigation of the Correlation Between Preoperative Diffusion Tensor Imaging Parameters and Histopathological Findings in Patients with Meningioma  
Enes Oğuzhan Alkan, Lutfullah Sarı, Serdar Balsak, Fatma Çelik Yabul, Fazılhan Altıntaş, Ganime Çoban

### CASE REPORTS

- 18 Partially Unroofed Coronary Sinus  
Jessi Cai, Cihan Duran
- 21 Sphenoidal Ectopic Adenohypophysis: A Rare Case Report and Literature Review  
İbrahim Feyyaz Naldemir, Ahmet Kürşat Karaman, Derya Güçlü

# A Review on the Medical Applications of Functional Magnetic Resonance Imaging

Bhagyalakshmi Akkavil Thondikandi<sup>1</sup>, Arun Krishnan MP<sup>2</sup>

<sup>1</sup>Department of Medical Physics and Radiation Safety, American Oncology Institute, Calicut, India

<sup>2</sup>Department of Medical Physics and Radiation Safety, MVR Cancer Center And Research Institute, Calicut, India

**Cite this article as:** Bhagyalakshmi AT, Arun KMP. A review on the medical applications of functional magnetic resonance imaging. *Current Research in MRI*. 2022; 1(1): 1-5.

**Corresponding author:** Bhagyalakshmi Akkavil Thondikandi, e-mail: bhagyalakshmiat@gmail.com

**Received:** June 1, 2022 **Accepted:** July 21, 2022

**DOI:** 10.5152/CurrResMRI.2022.221322



Content of this journal is licensed under a Creative Commons Attribution-NonCommercial 4.0 International License.

## Abstract

The ability to combine functional information with regular images will be a significant benefit and functional magnetic resonance imaging is an excellent example of such a tool. The development of functional magnetic resonance imaging has aided in the exact examination of brain function and identification of specific diseases. This review primarily focuses on similar advantages and achievements of functional magnetic resonance imaging procedure in a wide variety of fields, which becomes useful for the readers to urge further interest in this topic.

**Keywords:** BOLD, DWI, functional MRI

## INTRODUCTION

This article offers a review of functional magnetic resonance imaging's (fMRI) medical applications. Magnetic resonance imaging (MRI) is a technique that produces clear images of the human body by combining magnetism and radio waves. Nuclear magnetic resonance (NMR), a physics phenomenon discovered in the 1930s in which magnetic fields and radio waves induce atoms to emit small radio signals, is the basis for MRI. The first MRI test on a live human patient was done on July 3, 1977. Magnetic resonance imaging is a non-invasive approach for visualizing internal biological structures and detecting disease that detects atoms based on how they react in a magnetic field. Computed tomography (CT) is another frequent imaging technique that employs ionizing radiation and relies on the idea of differential attenuation of x-ray beams when they strike bones and soft tissues. The contrast variation among soft tissues is very difficult to identify in a CT scan, whereas MRI images give a superior demonstration of soft tissue contrast and use non-ionizing techniques. As a result, it is suitable for brain, spine, joint, and soft tissue body component inspections. Large amount of anatomical information can be derived from MRI scans; however, we found no information about the tissues' functional and physiological features. The necessity of imaging the functional aspects of tissues led to an intriguing new breakthrough in MRI termed as "functional MRI (fMRI)." Functional magnetic resonance imaging provides pictures of brain activity during task engagement that are not intrusive. Functional magnetic resonance imaging of the brain allows the visualization of active parts of the brain during certain activities and also helps in understanding their underlying networks. It measures the metabolic changes that occur within the brain and may be used to determine the parts of the brain that handles critical functions. The base for fMRI was established on the fact that local variations in cerebral blood flow, blood volume, and blood oxygenation are caused by neuronal activity. The breakthrough occurred when it was found that blood hemoglobin exhibits magnetic characteristics that differ from the amount of oxygen it carries. Oxy-hemoglobin has diamagnetic properties, while deoxyhemoglobin formed after the removal of oxygen has paramagnetic properties.<sup>1</sup> The presence of deoxyhemoglobin leads to the shortening of the T2\* relaxation time within the tissue voxel. These changes in the levels of oxygen in the blood will give varying MR signals. This effect of a small change in local MR signal is called the blood oxygen level-dependent effect (BOLD effect). Using visual and neural stimulus paradigms, this phenomenon was employed to create entirely non-invasive topographic maps of human brain activity.<sup>2</sup> In general, fMRI detects variations in blood flow to determine brain activity. It was concluded that the local differences in functional activity can change the vascular supply of the brain.<sup>3,4</sup>

Functional magnetic resonance imaging is a technology that compares pictures recorded during 2 states of a task: the ON state, when the subject performs a task (the activation state), and the OFF state, when the subject does not execute any activity (the baseline state). During the ON and OFF states, there is a change in the intensity of the images captured which are compared to obtain the mean difference in images, and then to get the activation maps, statistical significance tests are performed. This may be used for brain mapping, which is a collection of neuroscience procedures aiming at mapping biological quantities or qualities onto brain spatial representations, resulting in maps. Several neurological disorders demand functional information from the brain in addition to its structural details. Brain mapping methods can provide useful information on how the brain operates in both normal and pathological states. Functional magnetic resonance imaging used for brain mapping can be compared with other functional imaging methods such as optical imaging, single photon emission computed tomography, positron emission tomography (PET),

and magnetic encephalography. An overview of several brain mapping methodologies, as well as fMRI signal processing approaches, was given in the study by Daimiwal et al.<sup>5</sup> A single image does not provide any functional information; however, this may be investigated by varying the image intensity levels over time to get the needed functional information. These maps depict the brain areas responsible for a certain sensory or motor task and provide a clear image of neural activity that may be used to better understand brain function.<sup>5</sup>

Resting-state fMRI is helpful for kids or adults who struggle with difficult cognitive activities including decision-making, memory, attention, judgment, etc. Some of the methods used for analysis include neural networks, seed-based methods, graph methods, clustering algorithms, independent component analysis, and pattern classifiers.<sup>6</sup> In the absence of any stated task, distinct parts of the sensorimotor system of the brain varied slowly and simultaneously. In resting-state fMRI, brain networks showed strong baseline activity that was reduced while individuals performed a range of cognitive activities. Resting-state fMRI is a relatively novel route for examining regional interactions in the absence of activities. It captures spontaneous low-frequency fluctuations (0.1 Hz) in the BOLD signal. Resting-state fMRI has clinical uses in presurgical planning for patients with brain tumors and epilepsy, and the technology may possibly play a role in delivering diagnostic and prognostic information for neurological and psychiatric illnesses in the future.<sup>7,8</sup>

Diffusion-weighted imaging (DWI) and fMRI are 2 more contrast mechanisms that have revolutionized the identification of the above-mentioned pathologic disorders. Cellular structures at microscopic levels can be characterized by the degree of diffusion in tissues, and any hindrance in the normal process caused by some abnormal pathological process can be well explained by diffusion-weighted fMRI (DfMRI). The grayscale pixel values in DWI are determined by the underlying diffusivity in voxels, with high-diffusion voxels appearing hypointense (e.g., cerebrospinal fluid) and low-diffusion voxels appearing hyperintense (e.g., acute stroke). The usual Brownian motion of water molecules is limited and slowed by the existence of cell membranes and other impediments. Diffusion-weighted functional magnetic resonance imaging shows a distinct response pattern in the visual cortex than BOLD-fMRI, according to studies. The DfMRI signal is consistently quicker at both the beginning and offset of the stimulus, implying that the DfMRI signal is more directly connected to neuronal activities than the hemodynamic response, that is the BOLD contrast.<sup>9</sup>

Over decades, fMRI has invaded several fields of research and we have attempted to cite briefly the areas of research, focusing wide range of readers.

## MAIN POINTS

- This review article delves into functional magnetic resonance imaging (fMRI) and how it's utilised in medicine.
- fMRI adds more functional information to a scan.
- The change in blood oxygen level with activation is used in Functional Magnetic Reference (fMRI).
- fMRI is used to locate the exact region of the brain that is accountable for each act.
- fMRI may be used to diagnose a variety of disorders and can also be utilised in radiotherapy to segment normal tissue.

## Psychiatry

The development of fMRI methods has made significant advances to our understanding of the brain mechanisms underlying mental disorders. Mental disease is generally related to variations in the overall organization of functional communication “throughout” the brain network, according to Zhan et al.<sup>10</sup> A comparable research using neuroimaging in psychiatric patients found that any changes in thinking patterns, beliefs, feelings, or behaviors that occur during psychotherapy therapies can result in a normalization of functional brain activity at a global level.<sup>11</sup> Another research looked at the impact of the cognitive pragmatic treatment, a rehabilitation program (CPT), where a patient fMRI was taken before and after the treatment and the patient's behavioral improvements appeared to be supported by functional alterations at the cerebral level.<sup>12</sup> Functional magnetic resonance imaging also pointed out the significance of psychological therapy over pharmacological therapy through a study on seriously disabled group of patients with schizophrenia.<sup>13</sup>

## Affective Science

Functional magnetic resonance imaging has a great role in affective science which is the scientific study of emotion or affect. Studies were conducted with the understanding that the human voice is one of the most important means of social and emotional communication. It was found that specific portions of the brain were activated more on listening to a cheerful voice rather than an enraged tone. The study also discovered that only when accompanied by joyful features, cheery sounds were associated with greater activity in an unusual region.<sup>14</sup> It was found that neuronal activations occurred at different specific regions of the brain when the experimental fMRI was performed by inducing emotions.<sup>15</sup> Similar studies were carried out on rejection<sup>16</sup> and lie detection.<sup>17</sup>

## Alzheimer's Disease

Functional magnetic resonance imaging studies were carried out on patients with Alzheimer's disease to evaluate the neural basis for impaired semantic memory and it helped in obtaining results consistent with several other prior researches.<sup>18</sup> A few functional imaging studies have looked at the functional competence of certain brain areas and their links to Alzheimer's disease memory deficits.<sup>19</sup> It also assisted in distinguishing the brain responses in the early stages of Alzheimer's disease from normal aging. It aids early therapy by allowing researchers to explore changes in brain function linked to the initial indications of Alzheimer's disease in vivo, possibly before the occurrence of major irreparable structural damage.<sup>20</sup> Furthermore, research employing fMRI has revealed that following music therapy, the activation pattern of the brain during the processing of familiar and unfamiliar music was different in Alzheimer's disease patients.<sup>21</sup> Improvements in graph neural networks, as well as a novel Riemannian manifold-based model fMRI, can be utilized to diagnose Alzheimer's disease more efficiently.<sup>22</sup>

## Cancer

Small volumes of active tumor at the time of diagnosis and early disease recurrence can be detected using the novel imaging modality fMRI, which offers not only anatomic but also functional imaging. In addition to PET-CT now, fMRI has been proven to be a valuable tool for gynecologic cancer diagnosis. When PET-CT is more accurate in diagnosing ganglion disease, fMRI is more accurate in local preoperative staging.<sup>23</sup>

Another fMRI study was carried out between few controls and breast cancer patients to investigate the neuro-physiological differences during

visuospatial working memory. Activations in locations such as the inferior frontal gyrus, insula, thalamus, and midbrain were higher in breast cancer patients than in controls during working memory.<sup>24</sup> One of the fMRI studies found that incorporating BOLD-fMRI and diffusion tensor imaging into radiation treatment planning for high-grade gliomas near the primary motor cortex and corticospinal tracts is beneficial because these structures are adjacent to the target volume and can be clearly identified as organ at risks and spared during treatment.<sup>25</sup> A similar research looked at the use of fMRI for target delineation and key organ avoidance in brain radiation and found that it helped to identify and avoid functionally significant locations when developing treatment regimens.<sup>26</sup> In order to routinely adopt fMRI in clinical practice, an examination to check the reproducibility of the technique was performed on primary motor cortex as a way of providing margins of error for the radiotherapy planning stage.<sup>27</sup> Although studies suggest the judicious use of fMRI to help with neurosurgery planning, intraoperative electrocortical mapping remains the gold standard for locating the eloquent cerebral cortex.<sup>28</sup> Another research compares a careful review of morphological MRI data to the possible diagnostic advantages of presurgical fMRI. When compared to a highly deep investigation of structural 3-dimension MRI, routine presurgical fMRI provides for a superior assessment of the spatial link between brain tumor and motor cortex, greatly improving preoperative risk-benefit assessment and function-preserving surgery.<sup>29</sup> New functional glioma biomarkers that might help with diagnosis, treatment, and outcome prediction may come from fMRI.<sup>30</sup>

### Other Clinical Findings

Migraine is linked to abnormal intrinsic functional activity in the limbic and primary sensory systems, according to resting-state fMRI data.<sup>31</sup> An fMRI scan was used to compare pre- and post-treatment functional connectivity, and the results indicated substantial differences.<sup>32</sup> One of the studies also showed that acupuncture might help chronic stroke patients with aphasia recover their language.<sup>33</sup> and acute low back pain patients<sup>34</sup> where the neural mechanisms of the brain associated with acupuncture were studied using fMRI. McPherson et al<sup>35</sup> investigated the relationship between neural systems involved in creativity and those engaged in emotion, and their findings reveal that emotions have a strong influence on activity in prefrontal and other brain networks involved in creativity. An fMRI study was conducted to investigate the neural substrates underlying the human–pet relationship, and it was discovered that mothers rated the images of their child and dog as eliciting similar levels of excitement and pleasantness but that the ratings of their dog were also positively correlated with ratings of their dog's attachment.<sup>36</sup> Several fMRI studies were carried out to investigate the effect of music and emotions, where they established significant correlations.<sup>37</sup> The fMRI study of connectivity between the neuronal networks of the brain allows for a better understanding of epileptogenesis, insomnia disease, and human speech articulation.<sup>38-40</sup> When depressed patients were analyzed for suicidal behavior, it was commonly observed that there occurred reduced perfusion of the pre-frontal cortex, and the suicide attempters' social perception was linked to long-term neurological dysfunctions.<sup>41</sup> Even studies were carried out to examine the response of children's brains to food and common logos, and it was observed that the responses activated some brain regions when culturally familiar logos were viewed.<sup>42</sup> Also, a market survey was carried out to establish the liking of consumers for green products, in which an MRI study gave a result which was in favor of green products, while fMRI study did not point out any such trend which was the actual reflection of purchase behaviors.<sup>43</sup> Functional magnetic resonance imaging can be used to measure the acute pharmacological rewarding and reduced anxiety effects in alcoholics.

Resting-state fMRI suggests that alcohol affects specific brain areas and may offer a neurological foundation for alcohol's effects on behavioral performance.<sup>44</sup> Alcohol impairs both driving behavior and brain functions linked to motor planning and control, goal-directedness, error monitoring, and memory, according to an fMRI research, making drunk drivers a huge public hazard.<sup>45</sup> Similar studies were carried out on the effect of marijuana smokers and other heavy smokers.<sup>46</sup> Another study shows the neural activity in the ventral striatum, an area of the brain that encodes feelings of subjective pleasure. Neural activity of the brain showed that there was more brain activation in the left hemisphere in the data obtained through fMRI techniques, and it can be useful in testing theories of investor behavior. It was observed that, at the moment, a subject issues a command to sell a stock at a gain, there is a sharp rise in the brain than in the right hemisphere on playing chess. Furthermore, fMRI demonstrated that the superior frontal lobes, parietal lobes, and occipital lobes were all activated bilaterally.<sup>47,48</sup> An fMRI research was used to examine the impact of block building games and board games on children's spatial skills, and it revealed that the block play group improved in response speed and accuracy. The brain alterations related to the 2 play regimens were evaluated using fMRI during a mental rotation task, which revealed an enhanced engagement of areas linked to spatial working memory and spatial processing memory following training.<sup>49</sup> Even a study on neural empathetic response of users to violent video games was carried out by Szyck et al using fMRI and found that the users were not much affected by these games in character shaping, and their research found that the effects of violent media on emotional processing can be severe and short-lived.<sup>50</sup> Using fMRI, Shirley et al<sup>51</sup> discovered which brain regions were engaged during the 3 phases of meditation compared to the control condition.

Despite the above-mentioned clinical findings, there is no baseline validation of contrast variations upon neuronal activation seen in fMRI images. A question on the credibility of fMRI signals aroused when Mr. Benneth in his poster presented the fMRI images of a dead salmon fish. The pictures of humans in different emotional states and neuronal activation occurred in the salmon's brain suggesting meaningful activities were shown. Analyses were conducted utilizing separate generally used statistical tests as evidence.<sup>52</sup>

### DISCUSSION

Functional magnetic resonance imaging has already been used to evaluate a variety of clinical functions of the human brain, detecting the onset of Parkinson's disease and noting the presence of disorders such as depression.<sup>53</sup> Selection of treatment modality is very crucial in the treatment of cancers as it helps in reducing the risks and improving the chances of cure. One of the major errors that occur in radiation therapy is the incorrect delineation of tumor volumes. Functional magnetic resonance imaging helps to evaluate the functional status of cells to be treated, and hence, physicians can accurately contour the diseased volumes. Other than clinical areas, the practice of taking fMRI images of the brain is spreading to areas of national security. At the time of employee screening, they are asked to get fMRI scan of the brain while performing cognitive tasks in order to check the feelings of the employee when certain extreme topics like racial prejudice, religious extremism, mental illness, psychopathology etc., come into the picture. It was concluded that it helped in lowering the risk of terrorist threats and preserving the rights of citizens.<sup>54</sup> The subject under examination in these cases and whoever participates in any research trial are usually healthy, but, the practical difficulty comes in the examination of sick patients who may have little capacity to perform any of the cognitive



tasks. The signals obtained will be succumbed to more noise. One main drawback of fMRI is the long scanning time because of the low sensitivity of BOLD signal. This will result in more subject motion during the scanning and reduction of statistical significance of the activation maps and increases the prevalence of false activations. Motion correction tools along with recent development in software development, artificial intelligence, prediction models, and usage of different coding languages solve this drawback, and faster and more accurate images are possible with fMRI.<sup>55-59</sup>

Changes in blood flow, blood volume, and oxygen utilization over time are another form of physiological noise. This component accounts for two-thirds of physiological noise, which is the primary source of overall noise. Noise may also be caused by erroneous brain activity, as well as variances in mental strategy and behavior between persons and tasks within a topic. Prior to scanning, even on certain trails, individuals are instructed on how to behave or react.<sup>60</sup>

Other than subject-dependent noise, there are other sources of noise like thermal noise and system noise. Hence, it becomes necessary to set remarkable threshold values for the signals under study. Too high value for threshold can lead to very low output data for evaluation and very low threshold value can lead to excess noise resulting in evaluating false-positive signals. The evidence for this has been given by Benneth et al<sup>61</sup> in his dead salmon study. The study actually points out the necessity for multiple comparison correction. Before this controversy in 2010, around 25%-40% of the studies published on fMRI were not using the corrected comparisons. The problem lies in the analyses which are often based on low-power, small sample studies. The same was criticized by Vul et al<sup>62</sup> in his Voodoo correlations in neuroscience.

There is a need to find multiple techniques other than BOLD to cross-compare the results collected till date. Blood oxygen level-dependent effect is a bit noisy and it influences the signals. It was seen that the magnetic properties of the tissues change with change in temperature, that is, in the case of the brain, its temperature changes with change in activity. The early oxidation of glucose boosts brain temperature, which is then lowered as cold blood enters. Internal contrast caused by temperature changes is difficult to assess, but it can be improved by utilizing exogenous agents such as thulium compounds. We would only offer additional internal contrasts like acidity/alkalinity (pH), calcium-sensitive agents, neuronal magnetic field, and Lorentz effect to calm readers' nerves. When brain cells become active, their acid/alkaline balance changes, resulting in contrast dependent on pH. This is done far too frequently with the help of a third party. Calcium-sensitive drugs increase the sensitivity of MRI to calcium concentrations, as calcium ions are frequently used as messengers in activated neurons' cellular signaling pathways. The magnetic and electric fields in neurons are measured through neuronal magnetic field contrast.<sup>63</sup> A critical evaluation of MRI signals combining different contrast mechanisms is indeed necessary to evaluate the signals. Evidences are yet to be established so as to eliminate the risks of evaluating false-positive signals.

## CONCLUSION

The application of fMRI is extensively wide from simple brain study to different medical and non-medical applications. There are different types of internal contrasts agents, and careful evaluation of subjects is necessary. In this study, basic principles and types and applications of functional MRI techniques are briefly introduced and reviewed. However, due to the limitation in length, the detail of each technique in-depth cannot be analyzed.

**Peer-review:** Externally peer-reviewed.

**Author Contributions:** Concept – B.A.T.; Design – B.A.T.; Materials – B.A.T.; A.K.M.P.; Writing – A.K.M.P.; Critical Review – B.A.T.

**Declaration of Interests:** The authors have no conflicts of interest to declare.

**Funding:** The authors declared that this study has received no financial support.

## REFERENCES

- Pauling L, Coryell CD. The magnetic properties and structure of hemoglobin, oxyhemoglobin and carbonmonoxyhemoglobin. *Proc Natl Acad Sci U S A*. 1936;22(4):210-216. [\[CrossRef\]](#)
- Kwong KK, Belliveau JW, Chesler DA, et al. Dynamic magnetic resonance imaging of human brain activity during primary sensory stimulation. *Proc Natl Acad Sci U S A*. 1992;89(12):5675-5679. [\[CrossRef\]](#)
- Ogawa S, Lee TM, Kay AR, Tank DW. Brain magnetic resonance imaging with contrast dependent on blood oxygenation. *Proc Natl Acad Sci U S A*. 1990;87(24):9868-9872. [\[CrossRef\]](#)
- Roy CS, Smart, and Charles S. Sherrington. *J Physiol*. 1890;11(1-2):85-158.17. [\[CrossRef\]](#)
- Daimiwal N, Sundhararajan M, Shriram R. Applications of fMRI for brain mapping. *arXiv Preprint ArXiv:1301.0001*. 2012.
- Lee MH, Smyser CD, Shimony JS. Resting-state fMRI: a review of methods and clinical applications. *AJNR Am J Neuroradiol*. 2013;34(10):1866-1872. [\[CrossRef\]](#)
- Drake CT, Iadecola C. The role of neuronal signaling in controlling cerebral blood flow. *Brain Lang*. 2007;102(2):141-152. [\[CrossRef\]](#)
- Soto-León V, Torres-Llacsá M, Mordillo-Mateos L, et al. Static magnetic field stimulation over motor cortex modulates resting functional connectivity in humans. *Sci Rep*. 2022;12(1):7834. [\[CrossRef\]](#); Sainburg LE, Little AA, Johnson GW, et al. Characterization of resting functional MRI activity alterations across epileptic foci and networks. *Cereb Cortex*. 2022. [\[CrossRef\]](#)
- Aso T, Urayama S, Fukuyama H, Le Bihan D. Comparison of diffusion-weighted fMRI and BOLD fMRI responses in a verbal working memory task. *Neuroimage*. 2013;67:25-32. [\[CrossRef\]](#)
- Zhan X, Yu R. A window into the brain: advances in psychiatric fMRI. *BioMed Res Int*. 2015;2015:542467. [\[CrossRef\]](#)
- Beauregard M. Functional neuroimaging studies of the effects of psychotherapy. *Dial Clin Neurosci*. 2014;16(1):75-81. [\[CrossRef\]](#)
- Gabbatore I, Bosco FM, Geda E, et al. Cognitive pragmatic rehabilitation program in schizophrenia: a single case fMRI study. *Neural Plast*. 2017;2017:1612078. [\[CrossRef\]](#)
- Penadés R, Segura B, Inganzo A, et al. Cognitive remediation and brain connectivity: a resting-state fMRI study in patients with schizophrenia. *Psychiatry Res Neuroimaging*. 2020;303:111140. [\[CrossRef\]](#)
- Morningstar M, Mattson WI, Nelson EE. Longitudinal Change in Neural Response to Vocal Emotion in Adolescence. *Soc Cogn Affect Neurosci*. 2022. [\[CrossRef\]](#)
- Tamam, Sofina, Ahmad AH, Kamil WA. Modelling brain activations and connectivity of pain modulated by having a loved one nearby. *AIP Conf Proc*. AIP Publishing LLC. 2018;1972(1).
- Eisenberger NI, Lieberman MD, Williams KD. Does rejection hurt? An fMRI study of social exclusion. *Science*. 2003;302(5643):290-292. [\[CrossRef\]](#)
- Farah MJ, Hutchinson JB, Phelps EA, Wagner AD. Functional MRI-based lie detection: scientific and societal challenges. *Nat Rev Neurosci*. 2014;15(2):123-131. [\[CrossRef\]](#)
- Saarienen A, Jääskeläinen IP, Harjunen V, Keltikangas-Järvinen L, Jasinskaja-Lahti I, Ravaja N. Neural basis of in-group bias and prejudices: A systematic meta-analysis. *Neurosci Biobehav Rev*. 2021;131:1214-1227. [\[CrossRef\]](#)
- Zhang Q, Huang Y, Yan M. The neural mechanism of memory encoding 2nd International Conference on Mental Health and Humanities Education (ICMHHE 2021). Atlantis Press; 2021.
- Weiner MW, Veitch DP, Aisen PS, et al. The Alzheimer's Disease Neuroimaging Initiative 3: continued innovation for clinical trial improvement. *Alzheimers Dement*. 2017;13(5):561-571. [\[CrossRef\]](#)
- Shahinfard E, Robin Hsiung G, Boyd L, Jacova C, Slack P, Kirkland K P4-042: An FMRI Study to investigate the benefits of music therapy in patients with Alzheimer's disease. *Alzheimers Dem*. 2016;12(7S\_Part\_21):1030. [\[CrossRef\]](#)



22. Ma J, Zhang Jilian, Wang Z. Multimodality Alzheimer's disease analysis in deep Riemannian manifold. *Inf Process Manag.* 2022;59(4):102965. [\[CrossRef\]](#)
23. Alvarez Moreno E, Jimenez de la Peña M, Cano Alonso R. Role of new functional MRI techniques in the diagnosis, staging, and followup of gynecological cancer: comparison with PET-CT. *Rad Res Pract.* 2012;2012:219546. [\[CrossRef\]](#)
24. Scherling CS, Collins B, Mackenzie J, Bielajew C, Smith A. Pre-chemotherapy differences in visuospatial working memory in breast cancer patients compared to controls: an fMRI study. *Front Hum Neurosci.* 2011;5:122. [\[CrossRef\]](#)
25. Wang M, Ma H, Wang X, et al. Integration of BOLD-fMRI and DTI into radiation treatment planning for high-grade gliomas located near the primary motor cortex and corticospinal tracts. *Radiat Oncol.* 2015;10(1):64. [\[CrossRef\]](#)
26. Chang J, Narayana A. Functional MRI for radiotherapy of gliomas. *Technol Cancer Res Treat.* 2010;9(4):347-358. [\[CrossRef\]](#)
27. Garcia-Alvarez R., Liney GP, Beavis A, Turnbull LW. Reproducibility of fMRI for the definition of functional margins in radiotherapy planning. *Garcia reproducibility.* <http://citeseerx.ist.psu.edu/viewdoc/download?doi=10.1.1.574.4154&rep=rep1&type=pdf>.
28. Smits M. Functional magnetic resonance imaging (fMRI) in brain tumour patients. *Eur Assoc NeuroOncology Mag.* 2012;2(3):123-128.
29. Guerfel M, Kouki S, Ben Abdallah N. Diagnostic benefits of presurgical fMRI in patients with brain tumours in the primary sensorimotor cortex. *Eur Congress of Radiology-ECR 2017 / C-3073; vol 2017.* <https://dx.doi.org/10.1594/ecr2017/C-3073>.
30. Ghinda DC, Wu JS, Duncan NW, Northoff G. How much is enough—can resting state fMRI provide a demarcation for neurosurgical resection in glioma? *Neurosci Biobehav Rev.* 2018;84:245-261. [\[CrossRef\]](#)
31. Li TQ, Wang Y, Hallin R, Juto JE. Resting-state fMRI study of acute migraine treatment with kinetic oscillation stimulation in nasal cavity. *NeuroImage Clin.* 2016;12:451-459. [\[CrossRef\]](#)
32. Perrin JS, Merz S, Bennett DM, et al. Electroconvulsive therapy reduces frontal cortical connectivity in severe depressive disorder. *Proc Natl Acad Sci U S A.* 2012;109(14):5464-5468. [\[CrossRef\]](#)
33. Ping W, et al. Effect of acupuncture plus conventional treatment on brain activity in ischemic stroke patients: a regional homogeneity analysis. *J Trad Chin Med.* 2017;37(5):650-658.
34. Shi Y, Liu Z, Zhang S, et al. Brain network response to acupuncture stimuli in experimental acute low back pain: an fMRI study. *Evid Based Complement Alternat Med.* 2015;2015:210120. [\[CrossRef\]](#)
35. McPherson MJ, Barrett FS, Lopez-Gonzalez M, Jiradejvong P, Limb CJ. Emotional intent modulates the neural substrates of creativity: an fMRI study of emotionally targeted improvisation in jazz musicians. *Sci Rep.* 2016;6(1):18460. [\[CrossRef\]](#)
36. Stoeckel LE, Palley LS, Gollub RL, Niemi SM, Evins AE. Patterns of brain activation when mothers view their own child and dog: an fMRI study. *PLoS One.* 2014;9(10):e107205. [\[CrossRef\]](#)
37. Lu J, Yang H, Zhang X, He H, Luo C, Yao D. The brain functional state of music creation: an fMRI study of composers. *Sci Rep.* 2015;5(1):12277. [\[CrossRef\]](#)
38. Christiaen E, Goossens MG, Raedt R, et al. Alterations in the functional brain network in a rat model of epileptogenesis: a longitudinal resting state fMRI study. *Neuroimage.* 2019;202:116144. [\[CrossRef\]](#)
39. Li Z, Chen R, Guan M, et al. Disrupted brain network topology in chronic insomnia disorder: a resting-state fMRI study. *NeuroImage Clin.* 2018;18:178-185. [\[CrossRef\]](#)
40. Zacà D, Corsini F, Rozzanigo U, et al. Whole-brain network connectivity underlying the human speech articulation as emerged integrating direct electric stimulation, resting state fMRI and tractography. *Front Hum Neurosci.* 2018;12:405. [\[CrossRef\]](#)
41. Serafini G, Pardini M, Pompili M, Girardi P, Amore M. Understanding suicidal behavior: the contribution of recent resting-state fMRI techniques. *Front Psychiatry.* 2016;7:69. [\[CrossRef\]](#)
42. Bruce AS, Bruce JM, Black WR, et al. Branding and a child's brain: an fMRI study of neural responses to logos. *Soc Cogn Affect Neurosci.* 2014;9(1):118-122. [\[CrossRef\]](#)
43. Vezich IS, Gunter BC, Lieberman MD. The mere green effect: an fMRI study of pro-environmental advertisements. *Soc Neurosci.* 2017;12(4):400-408. [\[CrossRef\]](#)
44. Zheng H, Kong L, Chen L, Zhang H, Zheng W. Acute effects of alcohol on the human brain: a resting-state FMRI study. *BioMed Res Int.* 2015;2015:947529. [\[CrossRef\]](#)
45. Meda SA, Calhoun VD, Astur RS, Turner BM, Ruopp K, Pearson GD. Alcohol dose effects on brain circuits during simulated driving: an fMRI study. *Hum Brain Mapp.* 2009;30(4):1257-1270. [\[CrossRef\]](#)
46. Lopez-Larson MP, Rogowska J, Yurgelun-Todd D. Aberrant orbitofrontal connectivity in marijuana smoking adolescents. *Dev Cogn Neurosci.* 2015;16:54-62. [\[CrossRef\]](#)
47. Raggett GM, Ceravolo MG, Fattobene L, Di Dio C. Neural correlates of direct access trading in a real stock market: an fMRI investigation. *Front Neurosci.* 2017;11:536. [\[CrossRef\]](#)
48. Li K, Jiang J, Qiu L, et al. A multimodal MRI dataset of professional chess players. *Sci Data.* 2015;2(1):150044. [\[CrossRef\]](#)
49. Newman SD, Hansen MT, Gutierrez A. An fMRI study of the impact of block building and board games on spatial ability. *Front Psychol.* 2016;7:1278. [\[CrossRef\]](#)
50. Szyck GR, Mohammadi B, Münte TF, Te Wildt BT. Lack of evidence that neural empathic responses are blunted in excessive users of violent video games: an fMRI study. *Front Psychol.* 2017;8:174. [\[CrossRef\]](#)
51. Telles S, et al. A fMRI study of stages of yoga meditation described in traditional texts. *J Psychol Psychother.* 2015;5(185):2161-0487.
52. Bennett CM, Miller MB, Wolford GL. Neural correlates of interspecies perspective taking in the post-mortem Atlantic Salmon: an argument for multiple comparisons correction. *Neuroimage.* 2009;47(suppl 1):S125. [\[CrossRef\]](#)
53. Timmer MHM, Sescousse G, van der Schaaf ME, Esselink RAJ, Cools R. Reward learning deficits in Parkinson's disease depend on depression. *Psychol Med.* 2017;47(13):2302-2311. [\[CrossRef\]](#)
54. Sahito F, Slany W. Functional Magnetic Resonance Imaging and the Challenge of Balancing Human Security with State Security. *arXiv Preprint ArXiv:1204.3543.* 2012.
55. Zaitsev M, Akin B, LeVan P, Knowles BR. Prospective motion correction in functional MRI. *Neuroimage.* 2017;154:33-42. [\[CrossRef\]](#)
56. Boutet A, Madhavan R, Elias GJB, et al. Predicting optimal deep brain stimulation parameters for Parkinson's disease using functional MRI and machine learning. *Nat Commun.* 2021;12(1):3043. [\[CrossRef\]](#)
57. Allen EJ, St-Yves G, Wu Y, et al. A massive 7T fMRI dataset to bridge cognitive neuroscience and artificial intelligence. *Nat Neurosci.* 2022;25(1):116-126. [\[CrossRef\]](#)
58. Yang S, Bie X, Wang Y, Li J, Wang Y, Sun X. Image features of resting-state functional magnetic resonance imaging in evaluating poor emotion and sleep quality in patients with chronic pain under artificial intelligence algorithm. *Contrast Media Mol Imaging.* 2022;2022:5002754. [\[CrossRef\]](#)
59. Saba T, Rehman A, Shahzad MN, Latif R, Bahaj SA, Alyami J. Machine learning for post-traumatic stress disorder identification utilizing resting-state functional magnetic resonance imaging. *Microsc Res Tech.* 2022;85(6):2083-2094. [\[CrossRef\]](#)
60. Ashby FG. *Statistical Analysis of fMRI Data.* Cambridge: MIT press; 2019.
61. Bennett CM, Wolford GL, Miller MB. The principled control of false positives in neuroimaging. *Soc Cogn Affect Neurosci.* 2009;4(4):417-422. [\[CrossRef\]](#)
62. Vul E, Harris C, Winkelman P, Pashler H. Voodoo correlations in social neuroscience. *Perspect Psychol Sci.* 2009;4(3):274-290. [\[CrossRef\]](#)
63. Truong T-K, Avram A, Song AW. Lorentz effect imaging of ionic currents in solution. *Journal of Magnetic Resonance.* 2008;191(1):93-99.

# Magnetic Resonance Imaging Findings of Lower Extremity Morel-Lavellée Lesions in Pediatric Patients: A Preliminary Study

Erdem Fatihoğlu<sup>1</sup>, Özlem Kadirhan<sup>2</sup>

Department of Radiology, Erzincan Binali Yıldırım University, Faculty of Medicine, Erzincan, Turkey

**Cite this article as:** Fatihoğlu E, Kadirhan O. Magnetic resonance imaging findings of lower extremity morel-lavellée lesions in pediatric patients: A preliminary study. *Current Research in MRI*. 2022; 1(1): 6-9.

**Corresponding author:** Ozlem Kadirhan, e-mail: ozlemkkadirhan@gmail.com

**Received:** March 11, 2022 **Accepted:** May 23, 2022

DOI: 10.5152/CurrResMRI.2022.220106



Content of this journal is licensed under a Creative Commons Attribution-NonCommercial 4.0 International License.

## Abstract

**Objective:** Morel-Lavellée lesions are the accumulation of fluid, blood, and debris caused by the decomposition of the skin and subcutaneous tissue after degloving trauma. This lesion is often located in the greater trochanter of the femur in adults. However, a small number of studies in pediatric patients have shown localization and signal differences. In this study, we aimed to describe the characteristic magnetic resonance imaging findings of Morel-Lavellée lesions located in the lower extremities in the pediatric patient group.

**Methods:** Patients who were diagnosed with subcutaneous fluid on lower extremity magnetic resonance imaging in pediatric patient groups were retrospectively reviewed from the hospital medical archive. Age, gender, trauma history, magnetic resonance imaging findings, and lesion contents were recorded.

**Results:** Thirteen patients between 10 and 18 years of age were included in the study. The most common localization was the knee, and all of the lesions in the knee were anteriorly located (11/13, 84.6%). In 10 patients, trauma was involved in the etiology, while the etiology of the remaining 3 patients was unknown. All of the lesions were thin-walled and most of them were ovoid (10/13, 76.9%).

**Conclusion:** Although Morel-Lavellée lesions are often described in the neighbors with the femur in adults, they should be considered in all localizations of the body that had a trauma. In the pediatric patient group, anterior knee involvement is frequently observed in the lower extremities and most of the patients regress with conservative treatment.

**Keywords:** closed degloving injury, lower extremity, Morel-Lavellée lesion, magnetic resonance imaging, pediatric

## INTRODUCTION

Morel-Lavallée lesions (MLLs) are lymphatic, blood, and debris accumulations caused by rubbing of the skin and subcutaneous adipose tissue separation after a forceful trauma. Victor-Auguste Morel-Lavallée initially identified it in the area of the bony protrusion in 1863. This lesion is most commonly seen in individuals in their third and fourth decades in the area of the greater trochanter of the femur. However, there is little information about these lesions in children, and they are usually published as single case reports.<sup>1,2</sup> As a result, the changes in signaling and localization between children and adults are still unclear. Because MLLs arise from the deep compartment of the subcutaneous adipose tissue, they contain intralesional fat and may thus be distinguished from hematoma and bursitis.<sup>3</sup>

While it is commonly seen in adults following a car collision, it is more commonly related to sports in children. Post-traumatic absorption is reduced in children because subcutaneous adipose tissue thickness is minimal.<sup>3</sup> As a result, this lesion has a high vulnerability. In this study, we aimed to describe the characteristic magnetic resonance imaging (MRI) findings of MLL in the lower extremity in the pediatric patient group.

## METHODS

Approval for this retrospective study was granted by the Institutional Review Board. Informed consent was waived because of the retrospective nature (ethics committee number: 34336249-604.01.02-E.30236, date: August 10, 2022, Erzincan Binali Yıldırım University).

Patients whose subcutaneous collection was seen in lower extremity MRI were retrospectively re-evaluated from the hospital medical archive between January 2010 and June 2018. The study comprised patients ranging in age from 0 to 18. Age, gender, trauma history, MRI findings, and the contents of the lesion were all documented.

Measurements were performed with routine images of a 1.5 Tesla MR system (Magnetom Aera, Siemens Healthcare, Erlanger, Germany) (proton-density (PD) - turbo spin-echo (TSE) fat-suppressed (FS)-TRA: field of view (FoV) read 180 mm, FoV phase 100%, slice thickness 4 mm, base resolution 320, Repetition Time (TR) 2870 ms, Time to Echo (TE) 30 ms, slice 25, dist factor 20%. T1-TSE-SAG: FoV read 180 mm, FoV phase 100%, slice thickness 4 mm, TR 444 ms, TE 9.7 ms, slice 23, dist factor 10%. PD-TSE-FS-SAG: FoV read 180 mm, FoV phase 100%, slice

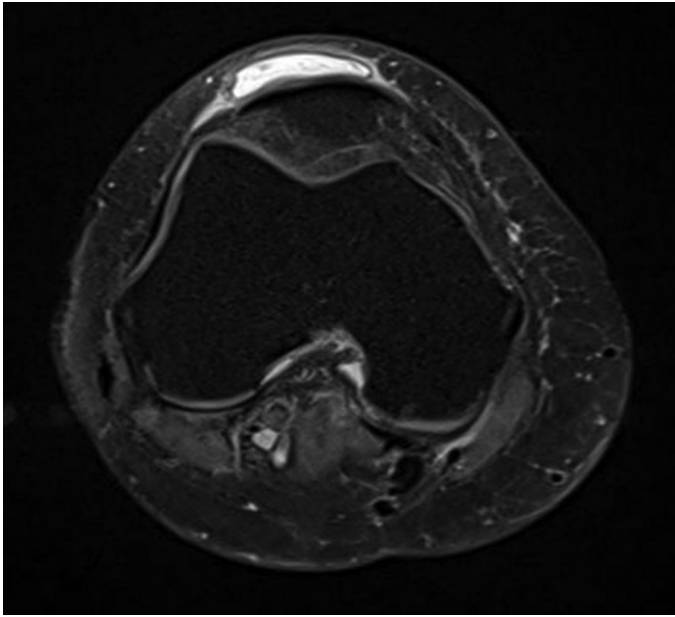


**Figure 1.** A 15-year-old male patient has a knee injury while playing basketball. Axial T2 fat-suppressed sequence, an ovoid, hyperintense subcutaneous collection with anterior medial retinaculum involvement is observed in the knee.

thickness 4 mm, TR 2700 ms, TE 38 ms, slice 25, dist factor 20%). Monitoring of fat deposits in a single section in the collections was considered sufficient to meet the Morel-Lavallée criterion (Figure 3).

The Statistical Package for the Social Sciences (SPSS) for Windows 20 (IBM SPSS Inc., Chicago, Ill, USA) tool was used to analyze the study data. The Kolmogorov–Smirnov test validated the data's normal distribution. The mean and standard deviation of normally distributed numerical data are displayed. The median is used to display data that does not have a normal distribution. To compare numerical variables between groups, the Student's *t*-test and the Mann–Whitney *U*-test were utilized. To explore any correlations between variables, Pearson's and Spearman's correlation analyses were utilized. The success of the diagnostic procedures studied was measured using positive predictive value, negative predictive value, and receiver operating characteristic analyses. A statistically significant value of  $P < .05$  was used.

### MAIN POINTS

- MLL are lymphatic, blood and rash accumulations caused by friction of the skin and separation of subcutaneous adipose tissue.
- Although MLL lesions are commonly seen after traffic accident-like severe trauma in adults, they have been identified in children mostly as a result of sports activities.
- The gold standard for the diagnosis of MLL is MRI.
- Since MLL lesions are caused by the deep division of subcutaneous adipose tissue, they can be distinguished from hematomas and bursitis due to the fact that they contain intralesional fat.
- MLL is most commonly seen in the anterior knee on the lower extremity in the pediatric population and presents as thin-walled and mostly oval.

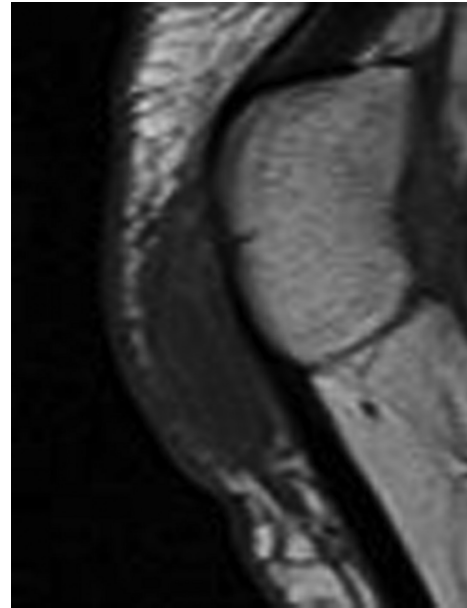


**Figure 2.** T1AG is hypointense and well-circumscribed since it does not contain hemorrhage.

### RESULTS

The study comprised 13 patients aged 10–18 years who had collections in their lower limbs and met the criteria. The average age was 15 years old. Septation was found in 9 (69%) of the lesions, with 10 patients being male and 3 patients being female (10/13, 76.9%). While there is an internal blood degradation product in three lesions (23%), there is none in others (Figure 2).

The orthopedics clinic referred 10 patients (10/13, 77%), while the pediatrics clinic referred 3 patients (3/13, 23%). On direct x-ray,

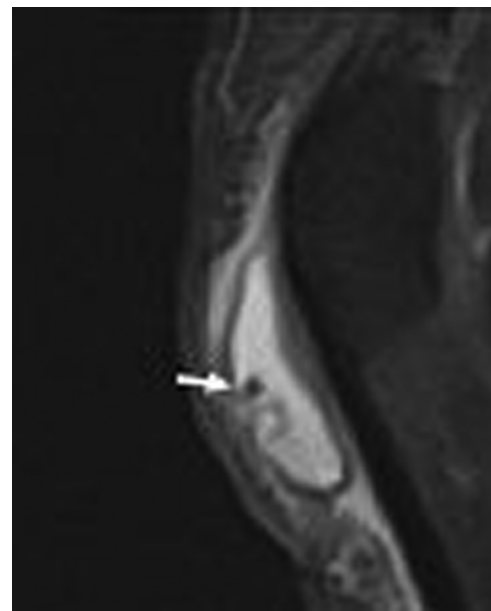


**Figure 3.** In the sagittal T2 fat-suppressed sequence, there is a fat droplet (white arrow) showing signal suppression secondary to the lipomatous content (figure 2 and figure 3 do not pass through the same section).



11 patients (11/13, 85%) had soft tissue edema, while 2 patients (2/13, 15%) had no findings. In all of the patients, there was no evidence of bone pathology.

The most common localization was the knee, and all lesions in the knee were anterior (11/13, 84.6%). Medial retinaculum was observed in 6 patients with anterior location (Figure 1), and lateral retinaculum location was observed in 5 patients. The other 2 patients had hip localization. While trauma was included in the etiology in 10 patients, the etiology of 3 patients was unknown. A history of sports-related trauma was found in 9 out of 10 patients (90%). The lesions were all thin-walled, with the majority of them being oval (10/13, 76.9%). In 9 cases (9/13, 69%), partial or complete capsule structure was seen. One knee lesion had a full-thickness anterior cruciate ligament rupture with bone marrow edema, while another had a medial retinaculum tear. Other lesions revealed no further abnormalities.

Only 1 patient (1/13, 8%) had a history of fine-needle aspiration and antibiotic treatment, while 12 patients (12/13, 92%) had a history of conservative care.

## DISCUSSION

Although prior classifications for MLLs recommended MRI categorization based on lesion morphology, presence of capsule, and general characteristics of the signal, it has not proven to be beneficial in the management and prognosis of MLL. As a result, no standardized application exists in this area.<sup>1,2</sup>

Although MLL lesions are commonly encountered in adults after severe trauma in a car accident, they have been described mostly in children in affluent countries as a result of sports activities such as football. The knee is the most common site of involvement, whereas the hip is the second most common site of involvement.<sup>1,4,5</sup>

Morel-Lavallée lesion may not be detected until there is a high level of clinical suspicion, and one-third of patients may be missed during the initial evaluation. As a result, pediatricians, general care providers, and sports medicine physicians should be aware of this diagnosis, particularly in young patients with sports injuries. A large suprapatellar palpable fluctuation area, frequently extending medially and laterally to the mid-femur, is the differentiating physical examination finding in MLL of the knee. Morel-Lavallée lesion of the knee can be distinguished from prepatellar bursitis and quadriceps contusions with a comprehensive history and thorough examination.<sup>1,4,5</sup>

There is very little information about pediatric MLL in the literature, and there are just 2 research on the subject. In a research by Rapp et al.<sup>3</sup> 21 patients were included, and lesions in the lower and upper extremities were examined in this investigation. In 19 cases, the most common localization was the knee. The lesion was described in the hip and proximal humerus in the remaining 2 cases. Furthermore, except for 2 lesions, all of the lesions in this investigation retreated spontaneously during follow-up, and the capsule structure was created 3 weeks after the shock. Due to a lack of clinical data, we were unable to calculate the duration between lesion formation and trauma in our investigation. As a result, its connection to capsule formation could not be determined. The healing time of the lesions could not be determined due to a lack of clinical data. Kushare et al<sup>1</sup> included 38 patients in their investigation, which focused solely on lower

extremity injuries, similar to ours. While 76% of lesions (29/38) were found below the knee, 24% (9/38) were found in the hip and pelvic region. In this regard, it is clear that this study, with a larger study population, is comparable to ours in terms of MLL distribution in the lower extremities.

In all of the literature, radiographs taken in patients with a history of trauma were described as normal, with the exception of soft tissue edema. This suggests that the injuries are mostly isolated soft tissue injuries and the doctor is probably trying to rule out any trauma-related bone anomalies.<sup>1,6,7</sup> The gold standard for diagnosing MLL is an MRI. Seroma, subacute hematoma, and chronic organized hematoma are the most prevalent components within the lesion, and they are hypointense on T1-weighted imaging and hyperintense on T2-weighted images. Ultrasound, which is the most common imaging modality for non-deeply placed MLL, has been indicated in several studies as a method of choice. However, because ultrasound examinations were performed on just a small percentage of the patients in our study, no assessment could be made in this area.<sup>7,8</sup>

In all but one of the patients in our investigation, a conservative treatment history was recorded, and in one of the patients, a history of aspiration with a minimally invasive surgery after antibiotic treatment was obtained. Although it is comparable to adults in terms of the absence of intervention, Kushare et al<sup>1</sup> said in his cohort study that a little more intervention was required in comparison to adults.<sup>5,9,10</sup> In this regard, there is some discrepancy between the 2 studies.

The hip is the most common location for lesions in adults in the literature, although the localization and signal characteristics of the knee are similar to those in our study. It will be better known when the lesion capsule is generated, how it regresses, and how the lesion signal features differ from the adult population if a cohort research is conducted with a bigger population in the literature.

## Limitations

Despite the fact that the number of patients in all trials is small, it is more prominent in ours. As a result, we had to work with a population that was too small to conduct extensive analysis. In this scenario, it created a statistical problem for us.

Some of the highly traumatized patients were unable to be identified with MLL because they regressed after receiving conservative care, with subcutaneous hematoma being considered after the fracture was ruled out in the emergency room. This condition made it impossible for us to expand our patient base.

Due to a lack of clinical information, the lesions could not be followed up.

## CONCLUSION

Morel-Lavallée lesions are typically recorded in adults close to the femur, but they should be evaluated in trauma patients in other locations of the body. The most common involvement in the lower extremities in pediatric patients is anterior knee involvement.

**Ethics Committee Approval:** Ethics committee approval for this study was obtained from the Ethics Committee of Erzincan Binali Yıldırım Üniversitesi Faculty of Medicine (Date: August 10, 2022, Decision No: 34336 249-6 04.01.02-E.3023).

All procedures performed in studies involving human participants were in accordance with the ethical standards of the institutional and/or national research committee and with the 1964 Helsinki declaration and its later amendments or comparable ethical standards.

**Peer-review:** Externally peer-reviewed.

**Author Contributions:** Concept – O.K., E.F.; Design – E.F.; Supervision – E.F.; Fundings – None; Materials – O.K., E.F.; Data Collection and/or Processing – O.K., E.F.; Analysis and/or Interpretation – O.K., E.F.; Literature Review – O.K., E.F.; Writing – O.K., E.F.; Critical Review Contribution Type – O.K., E.F.

**Declaration of Interests:** The authors declare that they have no competing interest.

**Funding:** This study received no funding.

## REFERENCES

1. Kushare I, Ghanta RB, Wunderlich NA. Morel-Lavallée lesions (internal degloving injuries) of the lower extremity in the pediatric and adolescent population. *Phys Sportsmed*. 2021;49(2):182-186. [\[CrossRef\]](#)
2. Harma A, Inan M, Ertem K. The Morel-Lavallée lesion: a conservative approach to closed degloving injuries. *Acta orthop traumatol turc*. 2004;38(4):270-273.
3. Rapp JB, Barrera CA, Ho-Fung VM. Morel-Lavallée lesions: MRI characteristics in the pediatric patient. *Pediatr Radiol*. 2019;49(4):559-565. [\[CrossRef\]](#)
4. Rai SK, Negi RS, Gogoi B, Kashid M. Morel-Lavallée lesion: an uncommon closed degloving injury that requires high index of suspicion and urgent attention. An experience of ten cases. *Sports Orthop Traumatol*. 2019;35(1):56-62. [\[CrossRef\]](#)
5. Divjak N, Kwiatkowski B, Tercier S. Morel-Lavallée lesion of the knee in the young athlete: about 2 cases after sports trauma. *Pediatr Emerg Care*. 2021;37(6):e354-e355. [\[CrossRef\]](#)
6. Singh R, Rymer B, Youssef B, Lim J. The Morel-Lavallée lesion and its management: a review of the literature. *J Orthop*. 2018;15(4):917-921. [\[CrossRef\]](#)
7. Borrero CG, Maxwell N, Kavanagh E. MRI findings of prepatellar Morel-Lavallée effusions. *Skelet Rad*. 2008;37(5):451-455. [\[CrossRef\]](#)
8. De Coninck T, Vanhoenacker F, Verstraete K. Imaging features of Morel-Lavallée lesions. *J Belg Soc Radiol*. 2017;101(suppl 2):15. [\[CrossRef\]](#)
9. Tejwani SG, Cohen SB, Bradley JP. Management of Morel-Lavallée lesion of the knee: twenty-seven cases in the national football league. *Am J Sports Med*. 2007;35(7):1162-1167. [\[CrossRef\]](#)
10. Anakwenze OA, Trivedi V, Goodman AM, Ganley TJ. Concealed degloving injury (the Morel-Lavallée lesion) in childhood sports: a case report. *J Bone Joint Surg Am*. 2011;93(24):e148. [\[CrossRef\]](#)

# Histopathological Correlation of Current Prostate Imaging Reporting and Data System Scores with 3 Tesla Multiparametric Prostate Magnetic Resonance Imaging in Detecting Prostate Cancer

Gökhan Tonkaz<sup>1</sup> , Düzgün Can Şenbil<sup>2</sup> 

<sup>1</sup>Department of Radiology, Erzurum City Hospital, Erzurum, Turkey

<sup>2</sup>Department of Radiology, Erzincan University, Faculty of Medicine, Erzincan, Turkey

**Cite this article as:** Tonkaz G, Şenbil DC. Histopathological correlation of current prostate imaging reporting and data system scores with 3 tesla multiparametric prostate magnetic resonance imaging in detecting prostate cancer. *Current Research in MRI*. 2022; 1(1): 10-14.

\*This study was produced from the academic thesis.

**Corresponding author:** Düzgün Can Şenbil, e-mail: senbilcan@gmail.com

**Received:** April 14, 2022 **Accepted:** May 8, 2022

DOI: 10.5152/CurrResMRI.2022.220510



Content of this journal is licensed under a Creative Commons Attribution-NonCommercial 4.0 International License.

## Abstract

**Objective:** This study aimed to evaluate the effectiveness of multiparametric prostate magnetic resonance imaging findings by scoring with the current guideline and correlating these scores with histopathology results in patients who underwent 3 T multiparametric prostate magnetic resonance imaging with the suspicion of prostate cancer and then underwent biopsy and/or radical prostatectomy.

**Methods:** Between January 2017 and January 2020, 399 patients who underwent imaging with the suspicion of prostate cancer and then biopsy due to elevated prostate specific antigen on the 3 T magnetic resonance imaging device were included in the study. Each patient's multiparametric prostate magnetic resonance imaging findings were scored independently by 2 readers using Prostate Imaging Reporting and Data System v2.1. We used appropriate statistical methods to examine the correlation between Prostate Imaging Reporting and Data System v2.1 scores and Gleason scores for 399 patients.

**Results:** The study included 399 patients ranging in age from 24 to 89 years; mean prostate specific antigen level was 17.2 ng/mL; mean prostate gland volume was 77.2 mL; and mean prostate specific antigen density was 0.35. Spearman correlation analysis revealed a positive correlation between the increase in Prostate Imaging Reporting and Data System v2.1 scores and the pathology Gleason scores.

**Conclusion:** In Prostate Imaging Reporting and Data System 1 or 2 lesions, biopsy should be avoided because the risk of clinically significant cancer is low. In Prostate Imaging Reporting and Data System 3 scores, the presence of clinically significant cancer is uncertain and biopsy is required because of suspicion of prostate cancer. Lesions classified as Prostate Imaging Reporting and Data System 4 or 5 have a high sensitivity, specificity, and negative predictive value for clinically significant cancer diagnosis. Histopathological examinations of these lesions should be performed.

**Keywords:** MpMRI, Prostate cancer, PIRADS

## INTRODUCTION

Prostate cancer is the most prevalent type of cancer in Europe's elderly male population and the second leading cause of death, after lung cancer.<sup>1</sup> Prostate cancer is a serious health problem in countries with a large elderly population. Around 1 in every 6 men will be diagnosed with prostate cancer at some point in their lives, and approximately 1 in every 36 men will die of prostate cancer.<sup>2</sup> The Gleason score and clinical stage at the time of diagnosis are the most important predictors of prognosis in prostate cancer. When prostate cancer is contained within the prostate gland at the time of diagnosis, there is a chance of cure; however, as the disease progresses, the cost of treatment increases. Additionally, it results in a high rate of mortality and morbidity.

Prostate cancer diagnosis is based on a combination of digital rectal examination, prostate specific antigen (PSA), and multiple prostate biopsy guided by transrectal ultrasonography (TRUS).<sup>3</sup> The PSA test is not a specific test and may be above normal limits for reasons such as prostatitis, prostate biopsy, globe vesicle, ejaculation, and prostate massage, apart from prostate cancer. Additionally, a PSA level within normal range does not rule out prostate cancer. Transrectal ultrasonography-guided biopsy is not a targeted procedure and is associated with a high rate of false-negative results.<sup>4</sup> The current situation has prompted researchers to look for noninvasive methods that will reduce the number of biopsy procedures, which are invasive, assist in performing targeted biopsies, and even enable the diagnosis of prostate cancer without biopsy.

Magnetic resonance imaging (MRI) has been used in this regard since the 1980s, especially in the last 10 years. The European Society of Urogenital Radiology published the "Prostate Imaging Reporting and Data System" (PIRADS) for the first time in 2012 to standardize image interpretation and reporting. Prostate Imaging Reporting and Data System version 2.1 (PIRADS v2.1) was published in 2019 as a result of research conducted in 2019.



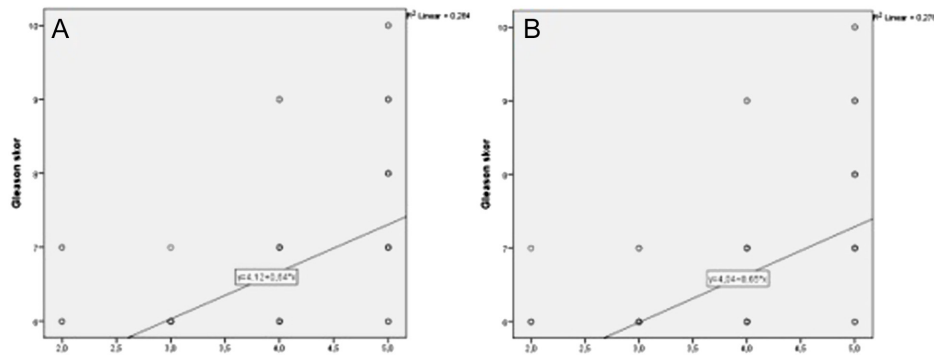


**Figure 1.** Correlation of PIRADS v2.1 score and Gleason score according to Readers 1 (A) and 2 (B).

The purpose of this study is to determine the correlation between PIRADS scores obtained in accordance with PIRADS v2.1 recommendations and the pathology results of prostate biopsy samples taken from patients with suspected prostate cancer who underwent MpMRI.

## METHODS

The Institutional Review Board approved this retrospective study (Protocol number: atauni-kaek-19-568, Atatürk University Faculty of Medicine, January 22, 2019). Because of the retrospective nature, informed consent was waived.

Between January 2017 and January 2020, patients who underwent 3T MRI imaging for prostate cancer screening due to an elevated PSA level at the Radiology Department of Atatürk University Medical Faculty Hospital were included in our study. A total of 532 patients who provided informed consent and underwent MR imaging were examined in our prospective study; 27 patients were excluded from the study due to a prior prostate cancer diagnosis, and 106 patients due to a lack of histopathological correlation. When the remaining imaging findings are analyzed, 399 patients underwent conventional 12-quadrant biopsy and/or radical prostatectomy. The relationship between the Gleason score derived from these patients' pathology results and the PIRADS score was investigated.

All prostate images in our study were acquired using a pelvic coil and axial-coronal-sagittal T2 weighted imaging (WI), axial diffusion weighted imaging (DWI), axial dynamic contrast examination, and pelvic postcontrast T1 WI to evaluate pelvic lymph nodes.

## MAIN POINTS

- The clinical behavior of prostate cancer can range from low-grade silent tumors that do not progress to invasive, aggressive fatal disease that progresses rapidly and becomes metastatic.
- Distinguishing the silent and aggressive forms of prostate cancer is very important in terms of treatment chances and management. Prostate specific antigen (PSA) and transrectal ultrasonography (TRUS)-guided biopsy is still the most widely used method for diagnosis. The PSA test is not a specific test. A TRUS-guided conventional biopsy is not a targeted examination and may miss the diagnosis of clinically significant cancer in a significant number of patients.
- Multiparametric prostate magnetic resonance imaging stands out as an imaging method that reduces overdiagnosis/overtreatment rates and can diagnose more clinically important cancers.

The prostate MR images were evaluated by a radiology assistant in her fourth year of education and a specialist radiologist with abdominal imaging experience, and the readers' compatibility was determined. Each patient was scored according to the PIRADS v2.1 guidelines. Following that, using an appropriate statistical method, the correlation between the double-blind PIRADS v2.1 scores and the Gleason scores obtained from the pathology was examined.

## Statistical Analysis

Standard deviation values were used to calculate patient ages, PSA values, and prostate volume mean. Cohen's kappa analysis was used to assess inter-investigator consistency in PIRADS scoring following MpMRI examination. The statistical analysis was performed using the Statistical Package for the Social Sciences 23.0 program (IBM SPSS Inc., Chicago, Ill, USA).

## RESULTS

The study included 399 patients aged 24-89 ( $63.1 \pm 9.3$ ); the mean PSA value was  $17.2 \pm 86.8$  ng/mL; the mean prostate gland volume was  $77.2 \pm 45.1$  mL; and the mean PSA density was  $0.35 \pm 2.3$ .

The Kappa value among readers was 0.826 for the PIRADS v2.1 scores of 399 patients who underwent histopathological examination. There was statistical significance ( $P = .01$ ) and significant agreement.

Spearman correlation analysis revealed a positive correlation between the increase in PIRADS v2.1 scores and the pathology Gleason scores. According to the first and second readers, the correlation value is 0.585 ( $P = .01$ ) and 0.579 ( $P = .01$ ), respectively (Figure 1).

Sixty-four (59.2%) of malignant lesions are located in the peripheral zone, 28 (26%) in the transitional zone, and 16 (14.8%) in both.

None of the ten PIRADS 1 lesions described by Reader 1 had a pathology result of CSC. Clinically significant cancer was detected in 2 patients as a result of the pathology of 149 PIRADS 2 lesions. As a result of the pathology of 144 PIRADS 3 lesions, CSC was reported in 1 patient. Clinically significant cancer was detected in 14 patients as a result of the pathology of 67 PIRADS 4 lesions. Clinically significant cancer was detected in 25 patients as a result of the pathology of 29 PIRADS 5 lesions (Table 1).

No CSC were identified in the pathology report of Reader 2's 6 PIRADS 1 lesions. One CSC was reported as a result of pathology in 149 PIRADS 2 lesions, 2 CSCs were reported as a result of pathology

**Table 1.** Pathology Result Corresponding to PIRADS Scores and PIRADS Scores Described by Reader 1

Reader 1	PIRADS 1	PIRADS 2	PIRADS 3	PIRADS 4	PIRADS 5	Total
Other	10	147	143	53	4	357
CSC	0	2	1	14	25	42
Total	10	149	144	67	29	399

CSC, clinically significant cancer; PIRADS, Prostate Imaging Reporting and Data System.

**Table 2.** Pathology Result Corresponding to PIRADS Scores and PIRADS Scores Described by Reader 2

Reader 2	PIRADS 1	PIRADS 2	PIRADS 3	PIRADS 4	PIRADS 5	Total
Other	6	148	145	54	4	357
CSC	0	1	2	14	25	42
Total	6	149	147	68	29	399

CSC, Clinically significant cancer; PIRADS, Prostate Imaging Reporting and Data System.

in 147 PIRADS 3 lesions, 14 CSCs were reported as a result of pathology in 68 PIRADS 4 lesions, and 25 CSCs were reported as a result of pathology in 29 PIRADS 5 lesions (Table 2).

When those with Gleason 7 and higher scores according to the pathology result are grouped and evaluated as high-risk (PIRADS 4 and 5) and non-high-risk (PIRADS 1, 2 and 3) according to the PIRADS v2.1 score, the positive predictive value in the analysis of Reader 1 is 0.40, negative predictive value was 0.99, sensitivity 0.92, and specificity 0.84 (Table 3).

When those with Gleason 7 and above according to the pathology result were grouped and evaluated as high-risk and non-high-risk according to the PIRADS v2.1 scores, the positive predictive value was 0.40, the negative predictive value was 0.99, the sensitivity was 0.92, and the specificity was 0.83 in the analysis of Reader 2 (Table 4).

## DISCUSSION

Prostate cancer is the most frequently diagnosed type of cancer in men.<sup>5</sup> Digital rectal examination, serum PSA, and conventional

**Table 3.** Analysis of CSC and Other Lesions as a Result of Pathology According to Reader 1 for High-Risk or Non-High-Risk Lesions According to PIRADS v2.1

Reader 1	Not High Risk (PIRADS 1, 2, and 3)	High Risk (PIRADS 4 and 5)	Total
Others	300	57	357
CSC	3	39	42
Total	303	96	399

CSC, clinically significant cancer; PIRADS, Prostate Imaging Reporting and Data System.

**Table 4.** Analysis of CSC and Other Lesions as a Result of Pathology According to Reader 2 for High-Risk or Non-High-Risk Lesions According to PIRADS v2.1

Reader 2	Not High Risk (PIRADS 1, 2, and 3)	High Risk (PIRADS 4 and 5)	Total
Others	299	58	357
CSC	3	39	42
Total	302	97	399

CSC, Clinically significant cancer; PIRADS, Prostate Imaging Reporting and Data System.

12-quadrant TRUS-guided biopsy are all used to diagnose prostate cancer.<sup>6</sup> Although the PSA test is not specific for prostate cancer, its normal range does not exclude it.<sup>7</sup> While TRUS-guided biopsy is standardized, it is not a targeted examination and thus may result in overdiagnosis/overtreatment and miss the diagnosis of CSC in a significant proportion of patients.<sup>8</sup> Prognosis prediction for prostate cancer is critical for individualizing treatment and determining the applicability of more effective treatment methods. After radical prostatectomy, the histopathological features of the disease provide critical information for predicting the disease's prognosis. Correlations between the PIRADS scoring system and final histopathology may also provide prognostic information. Thus, MpMRI data can also be used as a prognostic factor and can actually be used to modify patient treatment with appropriate risk stratification.<sup>9</sup>

In a study by Chen et al.<sup>10</sup> the agreement of PIRADS v2 scores between readers ( $\kappa=0.74$ ) was found to be moderate. Similarly, there are additional studies in the literature that demonstrate moderate reader agreement.<sup>11-13</sup> Apart from these, when all lesions were considered in the study by Greer et al.<sup>14</sup> inter-reader agreement ( $\kappa=0.37$ ) was found to be weak. This situation may vary according to the readers' knowledge and experience. The Kappa value for PIRADS v2.1 scores among readers was 0.826 in our study. There was statistical significance ( $P=.01$ ) and significant agreement.

In the study published by Daun et al.<sup>15</sup> the area under the Receiver Operating Characteristic (ROC) curve between PIRADS v2 score and Gleason scores was found to be 0.79. In our study, similar to this study, the area under the ROC curve was found to be 0.81 (good) and 0.80 (good) according to the first and second reader, respectively.

According to current guidelines, PIRADS 1 and PIRADS 2 lesions have a very low/low risk of CSC. Clinically significant cancers were not detected in any of the 3 patients with a PIRADS 1 score and 33 patients with a PIRADS 2 score in a study of 137 patients with a PIRADS v2 score and histopathological result published in 2019 by Daun et al.<sup>15</sup> According to Park et al's study, CSC could not be detected in approximately one-third of patients using MpMRI prior to biopsy, and approximately 60% of missed cancers had a PIRADS score of 1 or 2. In this study, when the retrospective MpMRI was re-evaluated, it was stated that 63.6% of the lesions were normal or could not be reliably distinguished from other structures, but 71.4% of these tumors were CSC. Additionally, this study stated that missed CSCs were smaller in size than other lesions detected, and the pathology outcome was cancers of lower grade.<sup>16</sup> Along with inconsistent findings in the literature, Reader 1 identified 10 PIRADS 1 and 144 PIRADS 2 lesions in our study. While PIRADS 1 lesions were benign, 2 PIRADS 2 lesions were reported to be CSC. On the other hand, Reader 2 described 6 PIRADS 1 lesions and 144 PIRADS 2 lesions. While all PIRADS 1 lesions were found to be benign, 1 PIRADS 2 lesion was found to be CSC. Additionally, when MpMRI images were evaluated retrospectively in patients who were classified as PIRADS 1 and 2 by the readers and had a pathology result of CSC, no focus suggestive of prostate cancer could be detected in the prostate gland. The positive predictive value of Readers 1 and 2 was determined to be 0.16-0.16 for the diagnosis of PIRADS 1 and 2 lesions and CSC, respectively. The negative predictive value was determined to range between 0.98 and 0.99. Additionally, the sensitivity ranged between 0.95 and 0.97 and the specificity ranged between 0.43 and 0.43. Inter-reader agreement for lesion identification is significant ( $\kappa=0.82$  and  $P=.01$ ). The pathology result reported as CSC for lesions described by readers as PIRADS 1 and 2 indicates

lesions outside the PIRADS v2.1 criteria or outside MpMRI detection limits. Furthermore, because the PIRADS score 1 and 2 lesions included in this study were those with pathology following biopsy, and there were PIRADS 1 and 2 lesions excluded from the study due to a lack of pathology results, it should be considered that there will be a relative increase in those reported as CSC with pathology results.

According to the current guideline, PIRADS 3 lesions are those with an uncertain presence of CSC, making clinical management difficult. The probability of malignancy of PIRADS 3 lesions in the literature has been described between 6.5% and 34% in the published PRECISION study.<sup>17</sup> Schlenker et al published a study in 2019 in which they performed targeted prostate MR-TRUS fusion biopsy on 41 PIRADS 3 lesions using the PIRADS v2 scoring system and found that 6 of them were CSC.<sup>17</sup> In a 2017 study published by Osses et al.<sup>18</sup> only 1 of 29 PIRADS 3 lesions was diagnosed as CSC. In our study, Reader 1 described 144 PIRADS 3 lesions. Of these, only 2 (1.3%) came from CSC. Reader 2 described 147 PIRADS 3 lesions. Of these, only 2 (1.3%) were reported as CSC. According to Readers 1 and 2, the percentage of patients defined as PIRADS 3 and reported as CSC with pathology results is relatively low compared to the literature, but the probability of these lesions being CSC was found to be higher than PIRADS 1 and 2 lesions and lower than PIRADS 4 and 5 lesions.

PIRADS 4-5 lesions are lesions with high/very high CSC presence according to current guidelines. In a 2017 study published by Osses et al. 38 (45%) of 84 PIRADS 4 lesions had a pathology result of CSC. In the same study, 24 (66%) of 36 PIRADS 5 lesions had a pathology result of CSC.<sup>18</sup> The rates of CSC for PIRADS 4 and 5 lesions were found to be 43%-67% in a multicenter study published in 2020 by Kızılay et al.<sup>9</sup> Apart from these, CSC rates ranged from 34% to 45% for PIRADS 4 lesions and 67% to 84% for PIRADS 5 lesions in 3 separate studies.<sup>18-20</sup> According to reader 1, in our study, 14 (20.9%) of 67 PIRADS 4 lesions had a pathology result of CSC. According to Reader 2, 14 (20.6%) of 68 PIRADS 4 lesions had a pathology result of CSC. According to Readers 1 and 2, 25 (86.2%) of 29 PIRADS 5 lesions were diagnosed as CSC, which is consistent with the literature. The positive predictive value was 0.41, the negative predictive value was 0.98, the sensitivity was 0.72, and the specificity was 0.93 in a study conducted by Mathur et al<sup>21</sup> in 2019 using the PIRADS v2 score system. The positive predictive value of Readers 1 and 2 was found to be 0.40-0.40 in our study for the diagnosis of PIRADS 4 and 5 lesions and CSC, respectively. The negative predictive value was determined to range between 0.99 and 0.99. Sensitivity and specificity were 0.92-0.92 and 0.84-0.83, respectively. Although the data are similar to the literature, PIRADS 4-5 lesions are likely to be CSC.

There are few studies in the literature examining the correlation between PIRADS and Gleason scores, and the results are inconsistent.<sup>22,23</sup> There is a need for further research into the prognostic value of MpMRI by examining the correlation between current PIRADS scores and histopathological factors. As a result, it is critical to diagnose clinically significant lesions, to assess the disease stage at the time of diagnosis and to assess the risk of progression during disease management.

The primary limitation of our study is that we obtained biopsies using the conventional method and did not compare the lesion in one-to-one MRI to the result of targeted biopsy and/or radical prostatectomy. Additionally, by increasing the readership, the diagnostic values of PIRADS v2.1 scores can be investigated in greater detail based on reader experiences.

Although MpMRI is the most sensitive and specific noninvasive procedure for early detection, localization, grading, and staging of prostate cancer,<sup>24</sup> the contribution of MpMRI to clinical practice is still unclear<sup>9</sup> and deserves further evaluation.

## CONCLUSION

Multiparametric prostate magnetic resonance imaging does not yet have a high enough positive predictive value to be used in place of systemic biopsy alone. According to the current PIRADS guidelines, there are insufficient studies in the literature.

The radiology component of prostate cancer diagnosis consists of imaging quality, a PIRADS guide, and an experienced radiologist. It is obvious that the problem arising from any of these 3 is reflected in the quality of the report.

Currently, there is a need for imaging and diagnostic methods that decrease prostate cancer overdiagnosis/overtreatment rates and can detect more CSCs. Multiparametric prostate magnetic resonance imaging may fill a portion of this unmet need.

**Ethics Committee Approval:** Ethical committee approval was received from Atatürk University Faculty of Medicine Institutional Review Board (Date: January 22, 2019, Decision No: atauni-kaek-19-568).

**Informed Consent:** Written informed consent was obtained from all participants who participated in this study.

**Peer-review:** Externally peer-reviewed.

**Author Contributions:** Concept – G.T., D.C.Ş.; Design – D.C.Ş.; Supervision – G.T.; Materials – G.T., D.C.Ş.; Data collection – G.T.; Analysis – G.T.; Literature Review – G.T.; Writing – G.T., D.C.Ş.; Critical Review – D.C.Ş.

**Declaration of Interests:** The authors declare that they have no competing interest.

**Funding:** This study received no funding.

## REFERENCES

1. Arnold M, Karim-Kos HE, Coebergh JW, et al. Recent trends in incidence of five common cancers in 26 European countries since 1988: Analysis of the European Cancer Observatory. *Eur J Cancer*. 2015;51(9):1164-1187. [\[CrossRef\]](#)
2. Loggitsi D, Gyftopoulos A, Economopoulos N, et al. Multiparametric magnetic resonance imaging of the prostate for tumour detection and local staging: imaging in 1.5 T and histopathologic correlation. *Can Assoc Radiol J*. 2017;68(4):379-386. [\[CrossRef\]](#)
3. Ketelsen D, et al. Detection of bone metastasis of prostate cancer. Comparison of whole-body MRI and bone scintigraphy; Nachweis ossaeer Metastasen des Prostatakarzinoms. Vergleich der Leistungsfähigkeit der Ganzkörper-MRT und der Skelettszintigrafie. *RÖFO Fortschr Geb Röntgenstr N Bildgeb Verfahr*. 2008;180.
4. Levine MA, Ittman M, Melamed JJ, Lepor H. Two consecutive sets of transrectal ultrasound guided sextant biopsies of the prostate for the detection of prostate cancer. *J Urol*. 1998;159(2):471-5; discussion 475. [\[CrossRef\]](#)
5. Siegel RL, Miller KD, Jemal A. Cancer Statistics, 2017. *CA Cancer J Clin*. 2017;67(1):7-30. [\[CrossRef\]](#)
6. Emberton M. Is a negative prostate biopsy a risk factor for a prostate cancer related death? *Lancet Oncol*. 2017;18(2):162-163. [\[CrossRef\]](#)
7. de Rooij M, Hamoen EH, Fütterer JJ, Barentsz JO, Rovers MM. Accuracy of multiparametric MRI for prostate cancer detection: a meta-analysis. *AJR Am J Roentgenol*. 2014;202(2):343-351. [\[CrossRef\]](#)
8. Loeb S. When is a negative prostate biopsy really negative? Repeat biopsies in detection and active surveillance. *J Urol*. 2017. *Wolters Kluwer Philadelphia, PA*;197(4):973-974. [\[CrossRef\]](#)
9. Kızılay F, Çelik S, Sözen S, et al. Correlation of Prostate-Imaging Reporting and Data Scoring System scoring on multiparametric prostate



- magnetic resonance imaging with histopathological factors in radical prostatectomy material in Turkish prostate cancer patients: a multicenter study of the Urooncology Association. *Prostate Int.* 2020;8(1):10-15. [\[CrossRef\]](#)
10. Chen F, Cen S, Palmer S. Application of Prostate Imaging Reporting and Data System version 2 (PI-RADS v2): interobserver agreement and positive predictive value for localization of intermediate-and high-grade prostate cancers on multiparametric magnetic resonance imaging. *Acad Radiol.* 2017;24(9):1101-1106. [\[CrossRef\]](#)
  11. Purysko AS, Bittencourt LK, Bullen JA, Mostardeiro TR, Herts BR, Klein EA. Accuracy and Interobserver Agreement for Prostate Imaging Reporting and Data System, Version 2, for the Characterization of Lesions Identified on Multiparametric MRI of the Prostate. *AJR Am J Roentgenol.* 2017;209(2):339-349. [\[CrossRef\]](#)
  12. Flood TF, Pokharel SS, Patel NU, Clark TJ. Accuracy and interobserver variability in reporting of PI-RADS version 2. *J Am Coll Radiol.* 2017;14(9):1202-1205. [\[CrossRef\]](#)
  13. Druskin SC, Ward R, Purysko AS, et al. Dynamic contrast enhanced magnetic resonance imaging improves classification of prostate lesions: a study of pathological outcomes on targeted prostate biopsy. *J Urol.* 2017;198(6):1301-1308. [\[CrossRef\]](#)
  14. Greer MD, Shih JH, Lay N, et al. Interreader variability of prostate imaging reporting and data system version 2 in detecting and assessing prostate cancer lesions at prostate MRI. *AJR Am J Roentgenol.* 2019;212(6):1-8. [\[CrossRef\]](#)
  15. Daun M, Fardin S, Ushinsky A, et al. PI-RADS version 2 is an excellent screening tool for clinically significant prostate cancer as designated by the validated International Society of Urological Pathology criteria: a retrospective analysis. *Curr Probl Diagn Radiol.* 2020;49(6):407-411. [\[CrossRef\]](#)
  16. Park KJ, Kim MH, Kim JK, Cho KS. Characterization and PI-RADS version 2 assessment of prostate cancers missed by prebiopsy 3-T multiparametric MRI: correlation with whole-mount thin-section histopathology. *Clin Imaging.* 2019;55:174-180. [\[CrossRef\]](#)
  17. Schlenker B, Apfelbeck M, Armbruster M, Chaloupka M, Stief CG, Clevvert DA. Comparison of PIRADS 3 lesions with histopathological findings after MRI-fusion targeted biopsy of the prostate in a real world-setting. *Clin Hemorheol Microcirc.* 2019;71(2):165-170. [\[CrossRef\]](#)
  18. Osses DF, van Asten JJ, Kieft GJ, Tijsterman JD. Prostate cancer detection rates of magnetic resonance imaging-guided prostate biopsy related to Prostate Imaging Reporting and Data System score. *World J Urol.* 2017;35(2):207-212. [\[CrossRef\]](#)
  19. Felker ER, Lee-Felker SA, Feller J, et al. In-bore magnetic resonance-guided transrectal biopsy for the detection of clinically significant prostate cancer. *Abdom Radiol (NY).* 2016;41(5):954-962. [\[CrossRef\]](#)
  20. Venderink W, van Luijckelaar A, Bomers JGR, et al. Results of targeted biopsy in men with magnetic resonance imaging lesions classified equivocal, likely or highly likely to be clinically significant prostate cancer. *Eur Urol.* 2018;73(3):353-360. [\[CrossRef\]](#)
  21. Mathur S, O'Malley ME, Ghai S, et al. Correlation of 3T multiparametric prostate MRI using prostate imaging reporting and data system (PI-RADS) version 2 with biopsy as reference standard. *Abdom Radiol (NY).* 2019;44(1):252-258. [\[CrossRef\]](#)
  22. Bastian-Jordan M. Magnetic resonance imaging of the prostate and targeted biopsy, Comparison of PIRADS and Gleason grading. *J Med Imaging Radiat Oncol.* 2018;62(2):183-187. [\[CrossRef\]](#)
  23. Slaoui H, Neuzillet Y, Ghoneim T, et al. Gleason score within prostate abnormal areas defined by multiparametric magnetic resonance imaging did not vary according to the PIRADS score. *Urol Int.* 2017;99(2):156-161. [\[CrossRef\]](#)
  24. Mohammadian Bajgiran AM, Afshari Mirak S, Shakeri S, et al. Characteristics of missed prostate cancer lesions on 3T multiparametric-MRI in 518 patients: based on PI-RADSV2 and using whole-mount histopathology reference. *Abdom Radiol (NY).* 2019;44(3):1052-1061. [\[CrossRef\]](#)

# Investigation of the Correlation Between Preoperative Diffusion Tensor Imaging Parameters and Histopathological Findings in Patients with Meningioma

Enes Oğuzhan Alkan<sup>1</sup>, Lutfullah Sarı<sup>2</sup>, Serdar Balsak<sup>2</sup>, Fatma Çelik Yabul<sup>2</sup>, Fazılhan Altıntaş<sup>2</sup>,  
Ganime Çoban<sup>3</sup>

<sup>1</sup>Medical Student, Bezmialem Vakıf University, Faculty of Medicine, İstanbul, Turkey

<sup>2</sup>Department of Radiology, Bezmialem Vakıf University, Faculty of Medicine, İstanbul, Turkey

<sup>3</sup>Department of Pathology, Bezmialem Vakıf University, Faculty of Medicine, İstanbul, Turkey

**Cite this article as:** Alkan EO, Sarı L, Balsak S, Çelik Yabul F, Altıntaş F, Çoban G. Investigation of the correlation between preoperative diffusion tensor imaging parameters and histopathological findings in patients with meningioma. *Current Research in MRI*. 2022; 1(1): 15-17.

**Corresponding author:** Lutfullah Sarı, e-mail: drlutfullahsari@gmail.com

**Received:** April 30, 2022 **Accepted:** August 1, 2022

DOI: 10.5152/CurrResMRI.2022.220813



Content of this journal is licensed under a Creative Commons Attribution-NonCommercial 4.0 International License.

## Abstract

**Objective:** Our study aimed to investigate whether the tumor differs in terms of apparent diffusion coefficient and fractional anisotropy values, mitotic index, and Ki-67 proliferation index in cases with transitional and atypical meningioma.

**Methods:** Forty-five patients (14 male and 31 female; 57±13.98 years old) were assessed using magnetic resonance imaging and diffusion tensor imaging before surgery. Apparent diffusion coefficient and fractional anisotropy values of the tumor were determined. Patients with atypical meningioma were classified as group 1 and those with transitional meningioma were considered group 2. The relationship between fractional anisotropy, apparent diffusion coefficient, Ki-67 proliferation index, and mitotic index was evaluated. Fractional anisotropy and apparent diffusion coefficient values of atypical meningiomas and transitional meningiomas were compared. Mann–Whitney U-test was used to compare the groups.

**Results:** Significant differences were found between group 1 and group 2 in terms of mitotic index and Ki-67 proliferation index (respectively,  $P = .001$  and  $P = .000$ ). There was no statistically significant difference between group 1 and group 2 in terms of fractional anisotropy and apparent diffusion coefficient values. In group 1, there was a positive correlation between fractional anisotropy values and mitotic index ( $P = .02$ ,  $r = 0.421$ ). Also, a negative correlation was found between apparent diffusion coefficient values and mitotic index ( $P = .04$ ,  $r = -0.374$ ). A negative correlation was found between apparent diffusion coefficient values and Ki-67 proliferation index in group 2 ( $P = .009$ ,  $r = -0.614$ ).

**Conclusions:** In preoperative imaging, adding diffusion tensor imaging to conventional magnetic resonance imaging and measuring fractional anisotropy and apparent diffusion coefficient values to predict the grade of meningiomas can be a guide for treatment planning.

**Keywords:** Atypical meningioma, apparent diffusion coefficient, diffusion tensor imaging, fractional anisotropy, meningioma, transitional meningioma

## INTRODUCTION

Among primary intracranial tumors, meningiomas account for 13–26% of all cases.<sup>1</sup> Arachnoid cap cells are known to be the origin of meningiomas. Parasagittal area, convexity, falx, skull base, as well as the ridge of the sphenoid bone are some of the most common localizations for these lesions. There are several treatment options available such as stereotactic radiosurgery, conformal radiotherapy, surgery, or their combinations<sup>2</sup> although passive check out is usually advised in case of asymptomatic lesions of lesser caliber or when the patient is elderly. If the tumor shows significant size growth or invades important structures and starts to become symptomatic, treatment is indicated.

The number of mitoses, signs of necrosis as well as parenchymal invasion are the main components of histopathological meningiomas grading. Grade 1 transitional meningiomas, also known as mixed meningiomas, are known to have features of both meningothelial and fibrous meningioma. Grade 2 atypical meningiomas make up about 8% of all meningiomas.<sup>3</sup> Atypical meningiomas, on the other hand, constitute 20–25% of recurring meningiomas.<sup>4</sup>

Diffusion tensor imaging (DTI) provides information regarding the direction of diffusion as well as tissue microstructural integrity. The most widespread parameters for DTI evaluation are apparent diffusion coefficient (ADC) and fractional anisotropy (FA). The significance of FA values in meningioma follow-up and diagnosis remains a controversial issue.<sup>1</sup> Several different studies reported variable FA values about meningioma grade.<sup>1,5</sup> It is known that ADC values correlate with tumor cellularity and the Ki-67 proliferation index.<sup>1,6</sup> As far as we know, the number of studies evaluating the radiation effects on meningioma patients who underwent Gamma Knife radiosurgery (GKR) with respect to volume changes and DTI parameters is few.<sup>4</sup> Our study aimed to investigate whether the tumor differs in terms of ADC and FA values, proliferation index, and mitotic index in cases with transitional and atypical meningioma.

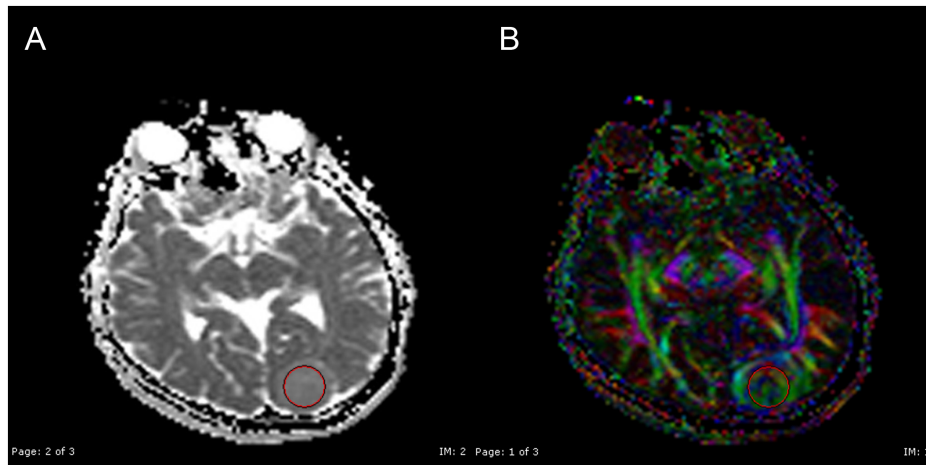


**Figure 1.** A 37-year-old woman with left occipital atypical meningioma. Apparent diffusion coefficient (A) and fractional anisotropy (FA) (B) values were calculated by placing region of interest that covers the tumor completely in FA maps.

## METHODS

The institutional ethics committee has approved our study (Date: 19 May, 2021, Decision No: 2021-16601). The data of the patients who were operated on with meningioma diagnosis between 2014 and 2020 at the Bezmialem University Hospital have been retrospectively gathered. Forty-five patients (14 male and 31 female;  $57 \pm 13.98$  years old) with meningioma treated with surgery were assessed using MRI and DTI preoperative. Fractional anisotropy and ADC values of the tumor were determined. Brain tissue invasion and the presence of 4 or greater mitoses have been accepted as the threshold for atypical meningioma diagnosis. Twenty-eight patients with atypical meningioma were classified as group 1 and 17 patients with transitional meningioma were considered group 2.

### Magnetic Resonance Imaging

Assessment of GKR treatment planning of the meningioma patients was done by a 1.5T MRI system (Avanto, Siemens, Erlangen, Germany). Following sequences of MRI were encompassed: coronal and axial fluid-attenuated inversion recovery (repetition time [TR]: 8000 ms, time echo [TE]: 90 ms, inversion time [TI]: 2500 ms), axial T1 (TR: 550, TE: 14 ms)-weighted images, axial and sagittal T2 TSE (TR: 4500, TE: 90 ms). Contrast (IV gadolinium-diethylenetriamine penta-acetic acid [Gd-DTPA]) T1 images in coronal, sagittal as well as axial planes were acquired. Three-dimensional T1 MPRAGE sequences with or without contrast were also included.

Following DTI parameters were used in the evaluation of the patients: single-shot SE echo-planar, TR/TE: 6000/89 ms; matrix,  $128 \times 256$ ;

FOV, 230 mm; spatial resolution, 1.54; and slice thickness, 5 mm. Diffusion-encoding in 30 separate aspects were obtained at  $b = 0 \text{ s/mm}^2$  and  $b = 1000 \text{ s/mm}^2$ . Obtained DTI information has been processed and FA maps were created on the workstation (Leonardo, Siemens, Erlangen, Germany). Fractional anisotropy and ADC values were quantified by manually positioning the elliptical regions of interest (ROI) within the tumor (Figure 1). Volumetric contrast 3D T1 MPRAGE images were taken as a reference when placing the ROI on the tumor. The dimensions of all ROIs were  $27.75 \pm 17.83 \text{ cm}^3$  (median,  $24 \text{ cm}^3$ ). The adaptation of the size and place of all ROIs within the tumor was implemented simultaneously by 2 radiologists. The association between FA, Ki-67 values, ADC proliferation index, and mitotic index was evaluated. Apparent diffusion coefficient and FA values of atypical meningiomas and transitional meningiomas were equated.

### Statistical Analysis

Shapiro–Wilk and Kolmogorov–Smirnov tests were used to determine if there is a normal distribution present. Fractional anisotropy and ADC points of atypical meningiomas and transitional meningiomas were equated. Mann–Whitney U-test was used to check our null hypothesis because of the total number one of the patient groups were smaller than 30 patients. The relationship between FA and ADC values, mitotic index, and Ki-67 was investigated by the Pearson correlation test. Statistical Package for the Social Sciences version 22.0. (IBM SPSS Corp.; Armonk, NY, USA) was used throughout the entire statistical analysis process.

## RESULTS

Both groups were compared in terms of the Ki-67 proliferation index and mitotic index, and significant differences were found (respectively,  $P = .000$  and  $P = .001$ ). There was no statistically meaningful disparity between atypical meningioma and transitional meningioma about ADC ( $P = .256$ ) and FA ( $P = .361$ ) values.

In group 1, a positive correlation was detected between mitotic index and FA values ( $P = .02$ ,  $r = 0.421$ ). As well, a negative correlation was detected between ADC values and mitotic index ( $P = .04$ ,  $r = -0.374$ ). A negative correlation was detected between Ki-67 proliferation index and ADC values in group 2 ( $P = .009$ ,  $r = -0.614$ ).

### MAIN POINTS

- Among primary intracranial tumors, meningiomas account for 13–26% of all cases.
- There are several treatment options available such as stereotactic radiosurgery, conformal radiotherapy, surgery, or their combinations.
- In preoperative imaging, adding diffusion tensor imaging to conventional magnetic resonance imaging and measuring fractional anisotropy and apparent diffusion coefficient values to predict the grade of meningiomas can be a guide for treatment planning.



## DISCUSSION

Diffusion tensor imaging provides useful information that can help us detect the abnormalities that meningiomas can have both before and after treatments such as radiosurgery.<sup>7-9</sup> Diffusion tensor imaging parameters provide important data on the level of microstructural damage and the behavior and organization of tumors according to their histological subtypes.<sup>6</sup> Fractional anisotropy quantifies anisotropic water diffusion and reveals its versatility and texture integrity. Fractional anisotropy gives salient details regarding the microorganization of fiber density, myelination, axon diameter, and white matter. Apparent diffusion coefficient separately quantifies the aspect of total water diffusion in textures and gives principal data regarding nucleus–cytoplasm ratio and tissue cellularity.<sup>1</sup> Despite the high sensitivity of FA and ADC in the differential diagnosis of high- and low-grade meningiomas, they do not furnish important details in the evaluation of microstructural texture alterations.<sup>1</sup> Compared to other types of meningiomas, fibroblastic meningiomas have been described as having relatively high FA and low ADC values.<sup>1</sup>

The evaluation of meningioma consistency could be navigated by FA values.<sup>10,11</sup> Due to the solid consistency of meningiomas, it is thought that isointensity in ADC maps and hyperintensity in FA maps are observed.<sup>10</sup> Apparent diffusion coefficient measurements contribute to determining the degree of meningioma.<sup>5,11,12</sup> There is a relationship between decreased tumor cellularity and increased ADC values.<sup>6</sup> It is thought that there may be a relationship between increased ADC values and decreased tumor cellularity.<sup>5,12</sup> Compared with fiber-rich fibroblastic meningiomas, meningiomas with a high proliferation index are more successfully treated with radiotherapy.<sup>6</sup> Long spindle-shaped tumor cells in meningiomas rich in fibrous tissue are predicted to own low ADC and high FA values because of their fascicular arrangement and increased content of interfascicular fibers.<sup>5,13-15</sup> It is speculated that fibroblastic meningiomas have a solid density may be due to their intracellular reticulin and collagen ingredient.

Due to the grade difference between atypical meningioma and transitional meningioma, significant differences were found when atypical meningioma and transitional meningioma were compared regarding the mitotic index and Ki-67 proliferation index. When comparing atypical meningioma and transitional meningioma regarding FA and ADC values, no substantial differences were seen between them. The number of patients is low and for this reason, it was thought that no statistically significant difference was detected. In group 1, a positive correlation was found between the mitotic index and FA values. Also, a negative correlation was found between the mitotic index and ADC values. In group 2, there was a negative correlation between the Ki-67 proliferation index and ADC values. The findings were thought to be compatible with the grade difference.

There are several limitations to our study. One of them is our study is a retrospective study. The other is the limited number of patients. Another major limitation is ROI placement, which is caused by the partial volume effect as a result of ROIs being placed in different locations. Diffusion tensor imaging values can be influenced by tumor heterogeneity.

## CONCLUSION

In preoperative imaging, adding DTI to conventional MRI and measuring FA and ADC values to estimate the grade of meningiomas can be a guide for treatment planning.

**Ethics Committee Approval:** Ethics committee approval was received for this study from the ethics committee of Bezmialem Vakıf University (Date: May 19, 2021, Decision No: 16601).

**Informed Consent:** Written informed consent was obtained from all participants who participated in this study.

**Peer-review:** Externally peer-reviewed.

**Author Contributions:** Concept – E.O.A., F.A.; Design – L.S.; Supervision – G.Ç., S.B.; Resources – S.B.; Materials – G.Ç., E.O.A.; Data Collection and/or Processing – E.O.A.; Analysis and/or Interpretation – F.C.Y.; Literature Search – F.C.Y.; Writing Manuscript – L.S., F.A.; Critical Review – G.Ç., L.S.; Other – F.A.

**Declaration of Interests:** The authors declare that they have no competing interest.

**Funding:** This study received no funding.

## REFERENCES

- Aslan K, Gunbey HP, Tomak L, Incesu L. The diagnostic value of using combined MR diffusion tensor imaging parameters to differentiate between low- and high-grade meningioma. *Br J Radiol.* 2018;91(1088):20180088. [\[CrossRef\]](#)
- Nguyen EK, Nguyen TK, Boldt G, Louie AV, Bauman GS. Hypofractionated stereotactic radiotherapy for intracranial meningioma: a systematic review. *Neurooncol Pract.* 2019;6(5):346-353. [\[CrossRef\]](#)
- Louis DN, Perry A, Reifenberger G, et al. The 2016 World Health Organization classification of tumors of the central nervous system: a summary. *Acta neuropathol.* 2016;131(6):803-820. [\[CrossRef\]](#)
- Kim JH, Kim YJ, Kim H, Nam SH, Choi YW. A rare case of transitional meningioma. *Arch Plast Surg.* 2015;42(3):375-377. [\[CrossRef\]](#)
- Wang S, Kim S, Zhang Y, et al. Determination of grade and subtype of meningiomas by using histogram analysis of diffusion-tensor imaging metrics. *Radiology.* 2012;262(2):584-592. [\[CrossRef\]](#)
- Speckter H, Bido J, Hernandez G, et al. Prognostic value of diffusion tensor imaging parameters for gamma knife radiosurgery in meningiomas. *J Neurosurg.* 2016;125(suppl 1):83-88. [\[CrossRef\]](#)
- Fatima N, Meola A, Pollom EL, Soltys SG, Chang SD. Stereotactic radiosurgery versus stereotactic radiotherapy in the management of intracranial meningiomas: a systematic review and meta-analysis. *Neurosurg Focus.* 2019;46(6):E2. [\[CrossRef\]](#)
- Ge Y, Liu D, Zhang Z, et al. Gamma Knife radiosurgery for intracranial benign meningiomas: follow-up outcome in 130 patients. *Neurosurg Focus.* 2019;46(6):E7. [\[CrossRef\]](#)
- Flannery T, Poots J. Gamma knife radiosurgery for meningioma. *Prog Neurol Surg.* 2019;34:91-99. [\[CrossRef\]](#)
- Huang RY, Bi WL, Weller M, et al. Proposed response assessment and endpoints for meningioma clinical trials: report from the Response Assessment in Neuro-Oncology Working Group. *Neuro Oncol.* 2019;21(1):26-36. [\[CrossRef\]](#)
- Romani R, Tang WJ, Mao Y, et al. Diffusion tensor magnetic resonance imaging for predicting the consistency of intracranial meningiomas. *Acta neurochir.* 2014;156(10):1837-1845. [\[CrossRef\]](#)
- Toh CH, Castillo M, Wong AM, et al. Differentiation between classic and atypical meningiomas with use of diffusion tensor imaging. *AJNR Am J Neuroradiol.* 2008;29(9):1630-1635. [\[CrossRef\]](#)
- Kashimura H, Inoue T, Ogasawara K, et al. Prediction of meningioma consistency using fractional anisotropy value measured by magnetic resonance imaging. *J Neurosurg.* 2007;107(4):784-787. [\[CrossRef\]](#)
- Tropine A, Dellani PD, Glaser M, et al. Differentiation of fibroblastic meningiomas from other benign subtypes using diffusion tensor imaging. *J Magn Reson Imaging.* 2007;25(4):703-708. [\[CrossRef\]](#)
- Speckter H, Bido J, Hernandez G, et al. Pretreatment texture analysis of routine MR images and shape analysis of the diffusion tensor for prediction of volumetric response after radiosurgery for meningioma. *J Neurosurg.* 2018;129(suppl1):31-37. [\[CrossRef\]](#)

# Partially Unroofed Coronary Sinus

Jessi Cai<sup>1</sup>, Cihan Duran<sup>2</sup>

Department of Diagnostic and Interventional Radiology, University of Texas, Health Science Center, Houston, USA

**Cite this article as:** Cai J, Duran C. Partially unroofed coronary sinus. *Current Research in MRI*. 2022; 1(1): 18-20.

**Corresponding author:** Cihan Duran, e-mail: cihan.duran@uth.tmc.edu

**Received:** May 18, 2022 **Accepted:** July 21, 2022

DOI: 10.5152/CurrResMRI.2022.221218



Content of this journal is licensed under a Creative Commons Attribution-NonCommercial 4.0 International License.

## Abstract

Unroofed coronary sinus is a rare congenital cardiac abnormality characterized by the partial or complete absence of the roof of the coronary sinus. Unroofed coronary sinus causes a shunt between the inferior left atrium and coronary sinus, which can lead to pulmonary hypertension and heart failure. Unroofed coronary sinus is typically associated with other congenital defects, most commonly a persistent left superior vena cava. We present the cardiac magnetic resonance imaging findings of a 6-year-old child with a rare unroofed coronary sinus requiring surgical closure.

**Keywords:** congenital heart disease, magnetic resonance imaging, unroofed coronary sinus

## INTRODUCTION

Unroofed coronary sinus (URCS) is a rare congenital cardiac defect characterized by an abnormal connection between the coronary sinus and the left atrium due to the partial or complete absence of the roof of the coronary sinus.<sup>1</sup> Unroofed coronary sinus is the rarest form of atrial septal defect (ASD). These defects may cause nonspecific clinical symptoms; however, accurate diagnosis is important as URCS has also been associated with the risk of pulmonary hypertension, brain abscess, or cerebral emboli.<sup>1,2</sup> We herein discuss the imaging of a child who required URCS closure at 6 years of age.

## CASE PRESENTATION

A 5-month-old Caucasian male infant with the diagnosis of an ASD, ventricular septal defect (VSD), and patent ductus arteriosus (PDA) had been referred for surgical repair due to failure to thrive with congestive heart failure symptoms. On post-operative day 2 after ASD/VSD closure and PDA ligation, he was found to be hypoxic with oxygen saturation in the low 80s on high fraction of inspired oxygen. Transthoracic echocardiogram

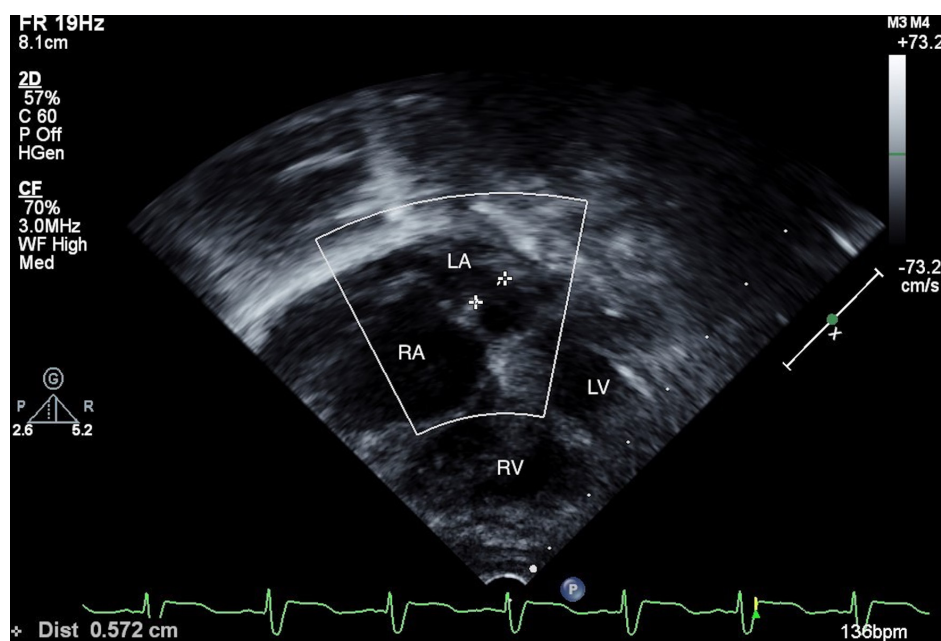


**Figure 1.** Transthoracic echocardiography demonstrating unroofed coronary sinus between (+) markers measuring 5.7 mm. LA, left atrium; RA, right atrium; LV, left ventricle; RV, right ventricle.

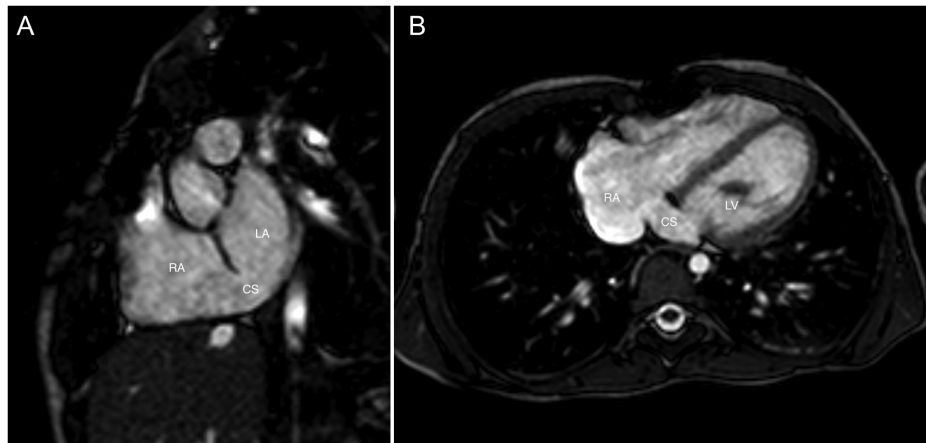


**Figure 2.** Cine balanced turbo field echo MR images in short axis view at the level of atrioventricular groove (A) and four-chamber (B) views show a dilated coronary sinus ostium with defect in the wall between the coronary sinus and left atrium. There is no PLSVC. LA, left atrium; RA, right atrium; CS, coronary sinus; PLSVC, persistent left superior vena cava.

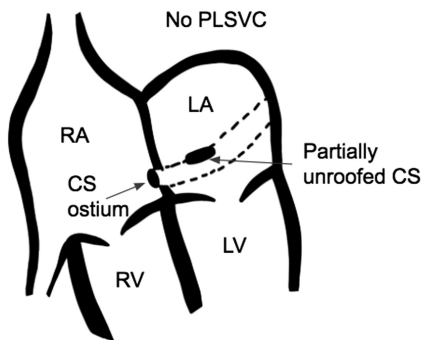


**Figure 3.** Schematic drawing of this case showing a type 3 partially unroofed mid-portion of the coronary sinus with no PLSVC. CS, coronary sinus; RA, right atrium; RV, right ventricle; LA, left atrium; LV, left ventricle; PLSVC, persistent left superior vena cava.

revealed a URCS with bidirectional shunting (Figure 1). Interventional cardiology performed right and left heart catheterization and angiography, which demonstrated unroofing of the mid-portion of the coronary sinus with drainage into the left atrium. There was no evidence of a persistent left superior vena cava (PLSVC).

At 6 years of age, the patient was referred to cardiovascular surgery for URCS closure due to a gradual increase in right ventricular pressure seen on sequential echocardiograms. Cardiac magnetic resonance imaging (MRI) was performed to further evaluate the previous findings for surgical planning. Cardiac spin-echo and cine MRI confirmed the previous findings of URCS with the absence of mid-portion of common wall between the coronary sinus and left atrium (Figures 2 and 3). Dilated coronary sinus ostium was measured at 10 mm. There

was mild dilatation of the right atrium and no significant dilatation of the right ventricle. Flow assessment by phase contrast velocity mapping measured  $Q_p : Q_s$  of 1.3 : 1. The patient underwent URCS closure with no intraoperative complications.

## DISCUSSION

Unroofed coronary sinus is a rare congenital cardiac anomaly characterized by a connection between the coronary sinus and the left atrium. It is the rarest form of ASD, representing less than 1% of all the ASDs.<sup>1</sup> The coronary sinus normally drains the cardiac veins into the right atrium (Figure 4). Unroofed coronary sinus is due to incomplete formation of the left atriovenous fold during embryonic development.<sup>4</sup> Isolated URCS, as in this patient, is rare as this defect has a strong association with a PLSVC, occurring in 75% of cases.<sup>1,3</sup>

Kirklin and Barratt-Boyes defined 4 types of URCS: type 1, completely unroofed with PLSVC; type 2, completely unroofed without PLSVC;

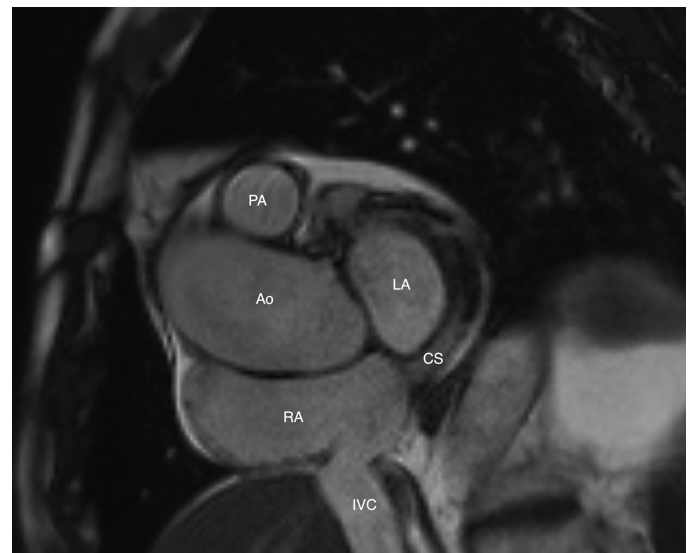


**Figure 4.** Cardiac MRI demonstrating normal coronary sinus draining into the right atrium. LA, left atrium; RA, right atrium; CS, coronary sinus; Ao, aorta; PA, pulmonary artery; IVC, inferior vena cava; MRI, magnetic resonance imaging.

## MAIN POINTS

- A rare case of unroofed coronary sinus requiring surgical closure was presented in this report.
- The importance of magnetic resonance imaging in diagnosis of unroofed coronary sinus was provided.
- Use of magnetic resonance imaging in surgical planning of unroofed coronary sinus was recommended.

type 3, partially unroofed mid-portion (as demonstrated in this case); and type 4, partially unroofed terminal portion.<sup>5,6</sup>

The symptoms associated with URCS are determined by the size of the defect and the degree of left-to-right shunting.<sup>1</sup> Clinical symptoms may range from asymptomatic to severe dyspnea with right-sided heart failure due to pulmonary hypertension.<sup>1</sup> Furthermore, because the coronary sinus is connected to the left atrium, there is a risk for paradoxical emboli such as cerebral abscesses.<sup>2</sup> Diagnosis of URCS is challenging because the clinical symptoms are nonspecific.

Prior to the use of advanced cardiac imaging, diagnoses such as URCS would only be possible during surgery or at autopsy. Although echocardiography is typically the first line in evaluating ASDs, the coronary sinus is a posterior structure that can be difficult to visualize.<sup>3</sup> Kim et al found echocardiography could easily visualize a dilated coronary sinus but not URCS in 5 out of 11 patients. Meanwhile, CT and MRI accurately demonstrated that all the patients had a defect in the coronary sinus.<sup>7</sup> Computed tomography and MRI are non-invasive imaging tests that have proven useful and more accurate in the diagnosis of URCS.<sup>3,4,7</sup>

When comparing CT and MR imaging for the diagnosis of URCS, both techniques have their advantages. Computed tomography imaging provides better anatomic information, but MRI shows high contrast resolution visualization of deep structures of the heart without the need for intravenous contrast or ionizing radiation.<sup>3</sup> With phase-contrast velocity-encoded cine technique, MRI also allows for flow measurement of the shunt created by URCS. This technique is performed on an imaging plane perpendicular to the long axes of the aorta and main pulmonary artery, then selecting the area of interest on cine images.<sup>7</sup> The ratio of pulmonary to systemic flow ( $Q_p : Q_s$ ) can then be calculated. Although flow information can also be obtained through cardiac catheterization, MRI is non-invasive and carries significantly fewer risks than a surgical procedure.

When evaluating for URCS on CT and MRI, the coronary sinus view, depicted by the cardiac short-axis view in the plane of the atrioventricular groove, provides the best visibility.<sup>7</sup> Both CT and MRI provide important 3D information about the anatomy of the URCS and play an important part in surgical planning.

Management of URCS is dependent on the severity of clinical symptoms. Transcatheter techniques are typically preferred over open-heart surgeries due to their less invasive nature.<sup>1</sup> Surgical repair of URCS

is performed by simple closure of the defect. In this case, the patient underwent successful open repair of the URCS.

## CONCLUSION

We present a rare case of URCS without PLSVC that required surgical closure in a 6-year-old child. Although echocardiography can aid in the diagnosis of URCS, cardiac MRI offers definitive diagnosis and high-resolution visualization of defects. Cardiac MRI provides important anatomical and flow measurement information that may be used in surgical planning, which can reduce the need for invasive procedures such as catheterization.

**Informed Consent:** Written informed consent was obtained from all participants who participated in this study.

**Peer-review:** Externally peer-reviewed.

**Author Contributions:** Concept – C.D.; Design – C.D., J.C.; Supervision – C.D.; Funding – none.; Materials – C.D., J.C.; Data Collection and/or Processing – C.D., J.C.; Analysis and/or Interpretation – C.D., J.C.; Literature Review – C.D., J.C.; Writing – C.D., J.C.; Critical Review – C.D., J.C.

**Declaration of Interests:** The authors declare that they have no competing interest.

**Funding:** This study received no funding.

## REFERENCES

1. Cintează EE, Filip C, Duică G, Nicolae G, Nicolescu AM, Bălgrădean M. Unroofed coronary sinus: update on diagnosis and treatment. *Rom J Morphol Embryol*. 2019;60(1):33-40.
2. Murthy A, Jain A, El-Hajjar M. Unroofed coronary sinus presenting as cerebral abscess: a case report. *Cardiol Res*. 2013;4(3):116-120. [\[CrossRef\]](#)
3. Shah SS, Teague SD, Lu JC, Dorfman AL, Kazerooni EA, Agarwal PP. Imaging of the coronary sinus: normal anatomy and congenital abnormalities. *RadioGraphics*. 2012;32(4):991-1008. [\[CrossRef\]](#)
4. Osei FA, Hill S, Shakti D. A rare congenital cardiac defect: isolated coronary sinus septal defect and the challenges of diagnosis in a child. *CASE (Phila)*. 2021;5(5):286-291. [\[CrossRef\]](#)
5. Bansal RC, Martens TP, Hu H, Rabkin DG. Unroofed coronary sinus discovered incidentally during cardiac surgery: systematic approach to diagnosis by transesophageal echocardiography. *CASE (Phila)*. 2021;5(6):384-391. [\[CrossRef\]](#)
6. Handa K, Fukui S, Kitahara M, Kakizawa Y, Nishi H. Minimally invasive surgical repair for unroofed coronary sinus syndrome directed by three-dimensional transesophageal echocardiography. *Surg Case Rep*. 2020;6(1):244. [\[CrossRef\]](#)
7. Kim H, Choe YH, Park SW, et al. Partially unroofed coronary sinus: MDCT and MRI findings. *AJR Am J Roentgenol*. 2010;195(5):W331-W336. [\[CrossRef\]](#)



# Sphenoidal Ectopic Adenohypophysis: A Rare Case Report and Literature Review

İbrahim Feyyaz Naldemir<sup>1</sup>, Ahmet Kürşat Karaman<sup>2</sup>, Derya Güçlü<sup>3</sup>

<sup>1</sup>Department of Radiology, Mardin Training and Research Hospital, Mardin, Turkey

<sup>2</sup>Department of Radiology, Süreyyapaşa Chest Diseases and Thoracic Surgery Training Hospital, İstanbul, Turkey

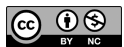
<sup>3</sup>Department of Radiology, Düzce University, Faculty of Medicine, Düzce, Turkey

**Cite this article as:** Naldemir İF, Karaman AK, Güçlü D. Sphenoidal ectopic adenohypophysis: A rare case report and literature review. *Current Research in MRI*. 2022; 1(1): 21-23.

**Corresponding author:** İbrahim Feyyaz Naldemir, e-mail: dr.ifnaldemir@gmail.com

**Received:** April 19, 2022 **Accepted:** June 21, 2022

**DOI:** 10.5152/CurrResMRI.2022.220914



Content of this journal is licensed under a Creative Commons Attribution-NonCommercial 4.0 International License.

## Abstract

The ectopic located pituitary gland is extremely rare, as in other congenital pituitary anomalies. This term refers to the location in the pharyngeal wall or sphenoid bone extending along the persistent craniopharyngeal canal. It occurs as a result of migration disorder of the adenohypophysis and may present with pituitary dysfunction or often accompany midline anomalies-related symptoms. Correct diagnosis of this rare ectopic location is important for the prevention of unnecessary surgery and surgical-induced panhypopituitarism. Here, we report a 41-year-old female patient with a pituitary gland located in the nasopharynx, which was detected incidentally in magnetic resonance imaging performed for neck pain.

**Keywords:** Craniopharyngeal canal, ectopic pituitary, magnetic resonance imaging

## INTRODUCTION

Congenital anomalies of the pituitary gland are rare. They may be accompanied by midline cranio-fascial anomalies. Intraspinal development of the anterior pituitary gland is also a very rare anomaly and is often asymptomatic. The reason for this anomaly is not clear.<sup>1</sup> In the literature, there are less than 10 cases related to this rare anomaly.<sup>2-4</sup> We aimed to present the adenohypophysis located in the nasopharynx through the persistent craniopharyngeal canal and the accompanying corpus callosum dysgenesis in this article.

## CASE PRESENTATION

A 41-year-old female patient was admitted due to increased neck pain at 4-month intervals. There was no medical history other than a major depressive disorder. Physical examination revealed cervical axis flattening and paravertebral muscle spasm. Neurological deficits and muscle weakness were not detected. Then, cervical magnetic resonance imaging (MRI) examination revealed no pathology except flattening of cervical lordosis. But the cross-section of the image area revealed a linear structure going from the sella turcica to the nasopharynx. Subsequently, in the pituitary MRI study performed later, it was seen that the anterior pituitary gland extended to the superior pharyngeal wall from the persistent craniopharyngeal canal (Figure 1). Ectopic localization of the pituitary gland was also seen on computed tomography (Figure 2).

Since there was no hormonal abnormality in the patient, imaging studies were considered to be most compatible with ectopic adenohypophysis owing to arrest of normal gland migration. In addition, dysgenesis of the corpus callosum was observed in the brain MRI study for additional anomaly screening.

## DISCUSSION

The pituitary gland is an organ of dual origin. The anterior lobe (adenohypophysis) is derived from oral ectoderm and is epithelial in origin, whereas the posterior lobe (neurohypophysis) derives from the neural ectoderm.<sup>5</sup> Adenohypophysis development in human begins with the formation of Rathke pouch in the fourth week. Rathke pouch (adenohypophyseal pouch) is formed by the funnel-shaped upward extension of the primitive oral roof lined with ectoderm. As the developmental steps progress, the adenohypophyseal pouch thickens, becomes elongated and eventually loses its connection with the primitive oral cavity in the seventh week. The 5 principal specialized endocrine cell types that form the pars distalis differ from the anterior wall of the pouch by the effect of various differentiation factors.<sup>6</sup>

Migration anomalies are congenital anomalies caused by genetic, vascular, or environmental insults to migrating neuroblasts. Exposure to ionizing radiation, excessive levels of alcohol (fetal alcohol syndrome), anticonvulsants (phenytoin and barbiturates), or toxic materials (methyl mercury poisoning) may be associated with abnormal neural cell migration.<sup>7</sup>

The persistence of the craniopharyngeal canal (CPC) is a corticated osseous canal that prolongs from the roof of the nasopharynx to the sellar region.<sup>7</sup> This canal, which traverses the sphenoid bone corpus, has also been named the transsphenoidal canal in the literature.<sup>8</sup> The incidence of

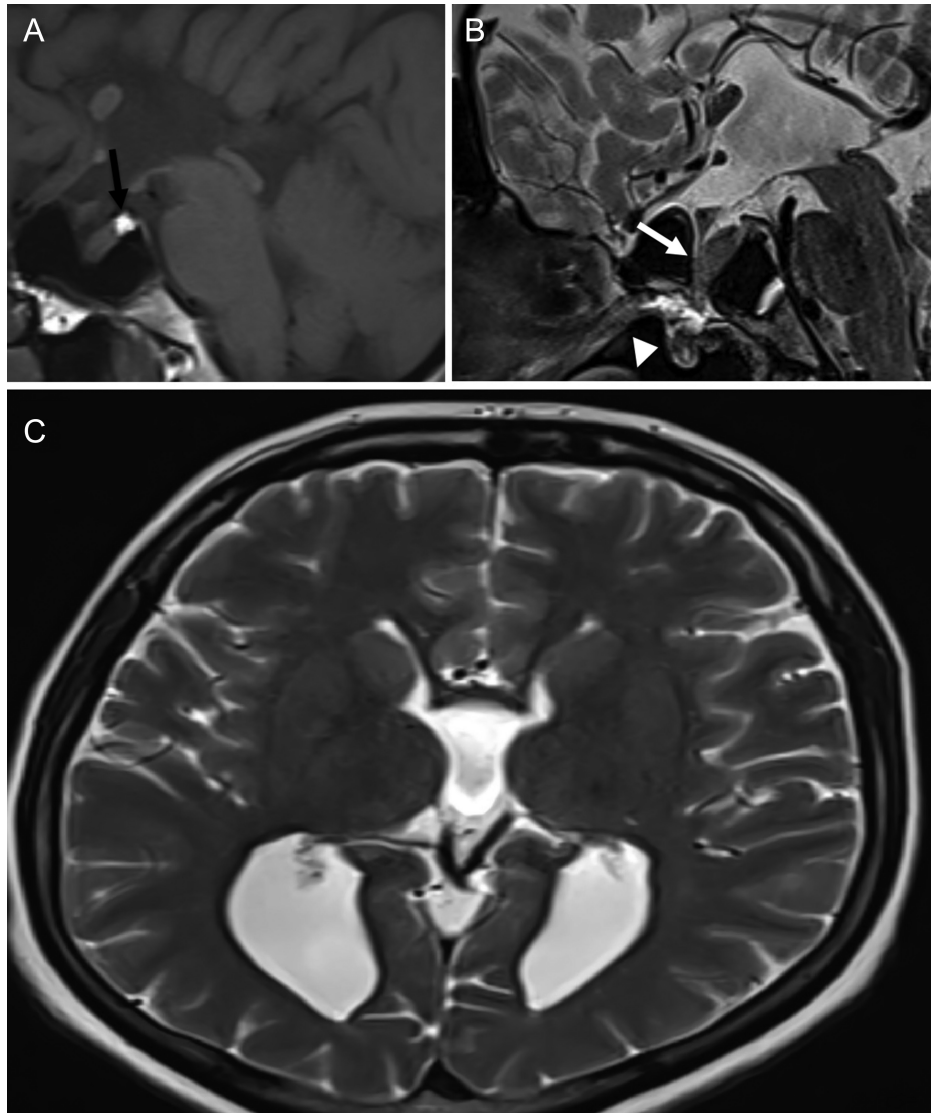


**Figure 1.** (A) Sagittal T1W, normally located neurohypophysis (black arrow). (B) The anterior pituitary gland extends from the persistent craniopharyngeal canal (white arrow) to the nasopharyngeal cavity (white arrowhead) and corpus callosum agenesis. In the sagittal T2W 3D-SPACE sequence (C) axial T2W, parallel configuration of the lateral ventricles and dilatation of the occipital horns secondary to corpus callosum agenesis. T1W, T1-weighted; T2W, T2-weighted.

CPC was reported as 0.42% in the population.<sup>9</sup> It is also stated that CPC may accompany many congenital anomalies. Parantez içerisindeki üstü çizili ifade metin içindeki atıfı belirtmekte olup buraya 8 ve 10 numaralı referansların “8,10” şeklinde eklenmesi uygun olacaktır. In

our case, there was ectopic adenohypophysis and corpus callosum dysgenesis accompanying CPC, similar to the literature.

Congenital anomalies of the adenohypophysis may be associated with other midline anomalies such as Chiari type 1 malformation, dysgenesis of the corpus callosum, and agenesis of the internal carotid artery.<sup>2,11</sup> Our patient having dysgenesis of the corpus callosum supported the hypothesis that this malformation may be associated with midline anomalies. It has been hypothesized that the relationship between congenital anomalies of adenohypophysis and other midline anomalies is related to fetal pituitary hormone deficiency.<sup>1</sup>

Ectopic intrasphenoidal pituitary gland is an extremely rare migration anomaly and refers to the ectopic location of the adenohypophysis in the nasopharyngeal wall or sphenoid bone. In both possibilities, CPC allows this ectopic location. Well-developed neurohypophysis can be in its normal position.<sup>1</sup> In our case, it is seen that the neurohypophysis is in its normal location. Therefore, persistent CPC plays

## MAIN POINTS

- Persistent craniopharyngeal canal is a rare midline anomaly that may be accompanied by adenohypophysis malformations.
- Ectopic adenohypophysis may cause hypopituitarism.
- Accurate diagnosis of ectopic adenohypophysis and description of anatomical structures can prevent important complications that may occur during surgical procedures.
- In patients with persistent craniopharyngeal canal and ectopic pituitary anomalies, other midline anomalies in the head and neck region should also be investigated.

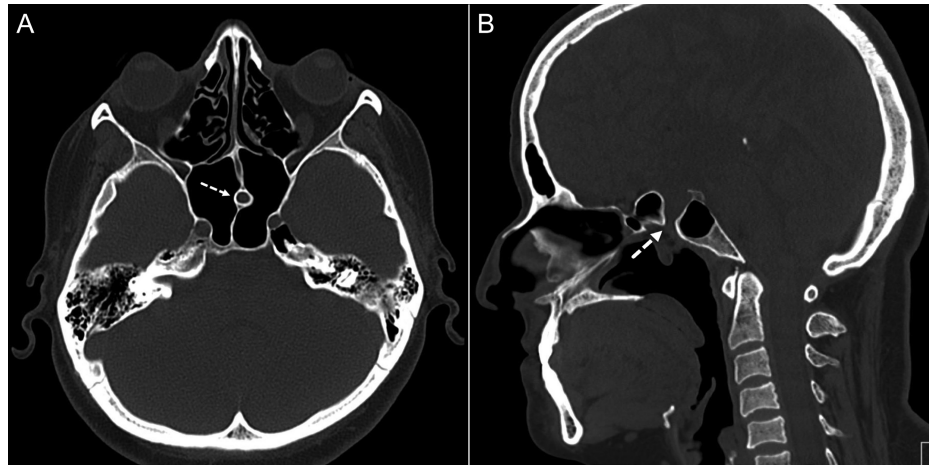


**Figure 2.** (A, B) CT (axial–sagittal), Persistent craniopharyngeal canal (dashed arrow) and protrusion of the adenohypophysis into the nasopharyngeal space. CT, computed tomography.

a key role in the occurrence of this anomaly. The CPC is believed to be due to the defective fusion in the postsphenoid cartilage and the non-obliteration of the adenohypophyseal stalk, which connects the adenohypophyseal pouch and the stomodeum.<sup>3,12</sup> In our case, the ectopic adenohypophysis was detected incidentally in the pharyngeal wall at the far end of the CPC and the neurohypophysis was in the intrasellar position. Abele et al<sup>3</sup> defined this as type 2 CPC which is characterized by the association of mid-sized CPC with ectopic pituitary tissue.

Various symptoms may be detected in cases of the ectopically located pituitary gland (type 2 persistent CPC). Pituitary displacement or surgical interventions may cause pituitary dysfunction.<sup>3,12,13</sup> Airway obstruction, accompanying symptoms related to hypothalamic hamartoma (hyperprolactinemia and precocious puberty), may be observed.<sup>12,14,15</sup> Also, it may present with symptoms and clinical findings related to other accompanying anomalies.<sup>1,3</sup> In our case, the diagnosis was made incidentally in an asymptomatic patient with significant pituitary displacement, and there was no hormonal abnormality. Therefore, a detailed evaluation in terms of pituitary function and other anomalies that may accompany these cases is important.<sup>3</sup> In addition, with the correct diagnosis, operation-related panhypopituitarism can be prevented by avoiding unnecessary surgery.<sup>4,13</sup> The causes of persistent CPC and ectopic hypophysis are still unclear and further studies are needed to find out the reasons that may prevent this malformation in the embryonic period. Clinical suspicion and early radiological evaluation (MRI) are required for accurate diagnosis and detection of other accompanying anomalies.

In conclusion, persistent craniopharyngeal canal and ectopic adenohypophysis are very rare variations and pathologies. Radiological evaluation is essential in the diagnosis and guiding treatment. The identification of these pathologies is of great importance in terms of preventing unnecessary surgery and possible complications.

**Informed Consent:** Written informed consent was obtained from the patient who participated in this study.

**Peer-review:** Externally peer-reviewed.

**Author Contributions:** Design – I.F.N., A.K.K., Supervision – D.G., Materials and Data Collection/Processing – I.F.N., D.G., Analysis/Interpretation and Literature Review – I.F.N., A.K.K., Writing – I.F.N., A.K.K., Critical Review – A.K.K.

**Declaration of Interests:** The authors declare that they have no competing interest.

**Funding:** This study received no funding.

## REFERENCES

1. Marsot-Dupuch K, Smoker WRK, Grauer W. A rare expression of neural crest disorders: an intrasphenoidal development of the anterior pituitary gland. *AJNR Am J Neuroradiol.* 2004;25(2):285-288.
2. Tijssen MPM, Poretti A, Huisman TAGM. Chiari type 1 malformation, corpus callosum agenesis and patent craniopharyngeal canal in an 11-year-old boy. *Neuroradiol J.* 2016;29(5):307-309. [CrossRef]
3. Abele TA, Salzman KL, Harnsberger HR, Glastonbury CM. Craniopharyngeal canal and its spectrum of pathology. *AJNR Am J Neuroradiol.* 2014;35(4):772-777. [CrossRef]
4. Esteban F, Ruiz-Avila I, Vilchez R, Gamero C, Gomez M, Mochon A. Ectopic pituitary adenoma in the sphenoid causing Nelson's syndrome. *J Laryngol Otol.* 1997;111(6):565-567. [CrossRef]
5. Amar AP, Weiss MH. Pituitary anatomy and physiology. *Neurosurg Clin N Am.* 2003;14(1):11-23, v. [CrossRef]
6. Dubois PM, El Amraoui A, Héritier AG. Development and differentiation of pituitary cells. *Microsc Res Tech.* 1997;39(2):98-113. [CrossRef]
7. Barkovich AJ, Chuang SH, Norman D. MR of neuronal migration anomalies. *AJR Am J Roentgenol.* 1988;150(1):179-187. [CrossRef]
8. Akyel NG, Alimlı AG, Demirkan TH, Sivri M. Persistent craniopharyngeal canal, bilateral microphthalmia with colobomatous cysts, ectopic adenohypophysis with Rathke cleft cyst, and ectopic neurohypophysis: case report and review of the literature. *Childs Nerv Syst.* 2018 July;34(7):1407-1410. [CrossRef]
9. Currarino G, Maravilla KR, Salyer KE. Transsphenoidal canal (large craniopharyngeal canal) and its pathologic implications. *AJNR Am J Neuroradiol.* 1985;6(1):39-43.
10. Habermann S, Silva AHD, Aquilina K, Hewitt R. A persistent craniopharyngeal canal with recurrent bacterial meningitis: case report and literature review. *Childs Nerv Syst.* 2021;37(2):699-702. [CrossRef]
11. Stagi S, Traficante G, Lapi E, et al. Agenesis of internal carotid artery associated with isolated growth hormone deficiency: a case report and literature review. *BMC Endocr Disord.* 2015;15(1):58. [CrossRef]
12. Hughes ML, Carty AT, White FE. Persistent hypophyseal (craniopharyngeal) canal. *Br J Radiol.* 1999;72(854):204-206. [CrossRef]
13. Weber FT, Donnelly WH Jr, Bejar RL. Hypopituitarism following extirpation of a pharyngeal pituitary. *Am J Dis Child.* 1977;131(5):525-528. [CrossRef]
14. Ekinci G, Kiliç T, Baltacıoğlu F, et al. Transsphenoidal (large craniopharyngeal) canal associated with a normally functioning pituitary gland and nasopharyngeal extension, hyperprolactinemia, and hypothalamic hamartoma. *AJR Am J Roentgenol.* 2003;180(1):76-77. [CrossRef]
15. Kizilkilic O, Yalcin O, Yildirim T, Sener L, Parmaksiz G, Erdogan B. Hypothalamic hamartoma associated with a craniopharyngeal canal. *AJNR Am J Neuroradiol.* 2005;26(1):65-67. Available at: <http://www.ajnr.org/content/26/1/65.abstract>.